



저작자표시-비영리-변경금지 2.0 대한민국

이용자는 아래의 조건을 따르는 경우에 한하여 자유롭게

- 이 저작물을 복제, 배포, 전송, 전시, 공연 및 방송할 수 있습니다.

다음과 같은 조건을 따라야 합니다:



저작자표시. 귀하는 원저작자를 표시하여야 합니다.



비영리. 귀하는 이 저작물을 영리 목적으로 이용할 수 없습니다.



변경금지. 귀하는 이 저작물을 개작, 변형 또는 가공할 수 없습니다.

- 귀하는, 이 저작물의 재이용이나 배포의 경우, 이 저작물에 적용된 이용허락조건을 명확하게 나타내어야 합니다.
- 저작권자로부터 별도의 허가를 받으면 이러한 조건들은 적용되지 않습니다.

저작권법에 따른 이용자의 권리는 위의 내용에 의하여 영향을 받지 않습니다.

이것은 [이용허락규약\(Legal Code\)](#)을 이해하기 쉽게 요약한 것입니다.

[Disclaimer](#)

A THESIS  
FOR THE DEGREE OF DOCTOR OF PHILOSOPHY

Anti-cancer effect of saringosterol acetate isolated from  
*Hizikia fusiforme* in zebrafish model

Eun-A Kim

Department of Marine Life Science  
GRADUATESCHOOL  
JEJU NATIONAL UNIVERSITY  
FEBRUARY, 2016

**Anti-cancer effect of saringosterol acetate isolated  
from *Hizikia fusiforme* in zebrafish model**

**Eun-A Kim**

**(Supervised by Professor You-Jin Jeon)**

A thesis submitted in partial fulfillment of the requirement for degree of

**DOCTOR OF PHILOSOPHY**

**2016.02**

This thesis has been examined and approved by



Thesis director, Choon Bok Song, Prof. of Marine Life Science



Kil-Nam Kim, Senior Researcher, Marine Bio Research Team



Seonheui Cha, Ph. D of School of Medicine, Ajou University



Soo-Jin Heo, Senior Researcher, Korea Institute of Ocean Science & Technology



You-Jin Jeon, Prof. of Marine Life Science

2016.02

**Department of Marine Life Science  
GRADUATE SCHOOL  
JEJU NATIONAL UNIVERSITY**

## CONTENTS

국문초록.....	v
<b>LIST OF FIGURES.....</b>	<b>ix</b>
<b>LIST OF TABLE.....</b>	<b>xxi</b>
<b>INTRODUCTION.....</b>	<b>1</b>
 <b>Part I . Saringosterol acetate of <i>Hizikia fusiforme</i> exhibits an anti-cancer effect in Hep3B and Du145 cell lines</b>	
 <b>ABSTRACT.....</b>	<b>13</b>
<b>MATERIALS AND METHODS.....</b>	<b>15</b>
<b>Chemicals and reagents.....</b>	<b>15</b>
<b>Preparation of crude extracts from <i>Hizikia fusiforme</i>.....</b>	<b>15</b>
<b>CPC process.....</b>	<b>15</b>
<b>ESI/MS analysis of purified compound.....</b>	<b>16</b>
<b><sup>1</sup>H-NMR and <sup>13</sup>C-NMR analysis of purified compound.....</b>	<b>16</b>

<b>Cell culture.....</b>	<b>16</b>
<b>LDH Cytotoxicity assay.....</b>	<b>17</b>
<b>Cell cycle analysis.....</b>	<b>18</b>
<b>Western blot analysis.....</b>	<b>18</b>
<b>Statistical analysis.....</b>	<b>19</b>
<b>RESULTS.....</b>	<b>20</b>
<b>DISCUSSIONS.....</b>	<b>29</b>
<b>CONCLUSION.....</b>	<b>30</b>
<b>Part II. Anti-liver cancer effect of saringosterol acetate in diethylnitrosamin- induced zebrafish embryos</b>	
<b>ABSTRACT.....</b>	<b>32</b>
<b>MATERIALS AND METHODS.....</b>	<b>34</b>
<b>Chemicals and reagents.....</b>	<b>34</b>
<b>Origin and maintenance of parental zebrafish.....</b>	<b>34</b>
<b>Experimental design of diethylnitrosamin (DEN)-induced cancer.....</b>	<b>35</b>
<b>Determination of ROS production.....</b>	<b>36</b>

<b>Determination of Cell death.....</b>	<b>36</b>
<b>Real-time PCR analysis.....</b>	<b>35</b>
<b>Western blot analysis.....</b>	<b>37</b>
<b>Statistical analysis.....</b>	<b>38</b>
<b>RESULTS.....</b>	<b>39</b>
<b>DISCUSSIONS.....</b>	<b>50</b>
<b>CONCLUSION.....</b>	<b>51</b>

**Part III. The potential anti-metastatic and anti-invasive effects of saringosterol acetate of *Hizikia fusiform* in liver and prostate tumor xenograft zebrafish models**

<b>ABSTRACT.....</b>	<b>53</b>
<b>MATERIALS AND METOHDS.....</b>	<b>55</b>
<b>Chemicals and reagents.....</b>	<b>55</b>
<b>Cell culture.....</b>	<b>55</b>
<b>Fluorescent cell labeling.....</b>	<b>55</b>
<b>Origin and maintenance of parental zebrafish.....</b>	<b>56</b>

<b>Experimental design of liver cancer cell xenograft.....</b>	<b>56</b>
<b>Determination of <math>\alpha</math>-fetoprotein(AFP) production and prostate-specific antigen(PSA) production analysis.....</b>	<b>57</b>
<b>Real-time PCR analysis.....</b>	<b>57</b>
<b>Western blot analysis.....</b>	<b>58</b>
<b>Histological analysis.....</b>	<b>59</b>
<b>Embryo preparation and tumor cell implantation.....</b>	<b>59</b>
<b>Statistical analysis.....</b>	<b>61</b>
<b>RESULTS.....</b>	<b>59</b>
<b>DISCUSSIONS.....</b>	<b>84</b>
<b>CONCLUSION.....</b>	<b>87</b>
<b>REFERENCES.....</b>	<b>88</b>
<b>ACKNOWLEDGEMENT.....</b>	<b>95</b>

## 국문 초록

제브라피쉬 (Zebrafish, *Danio rerio*)는 작은 열대성 담수어로써, 유전자정보 및 조직기관이 인간과 유사한 척추동물로 인간질환연구의 모델로써 높이 평가되고 있다. 특히 난이 작으며 투명하고 체외수정을 하여 해부현미경 하에서 쉽게 발생의 모든 과정을 관찰 할 수 있으며, DNA, RNA을 배아에 직접 주입가능, 특정세포의 라벨화, transplantation이 용이하여 RNA와 단백질 수준에서의 유전자 조절 연구를 손쉽게 할 수 있다. 초기 세포분열은 15분 간격으로 진행, 24시간이 지나면 심장의 박동과 혈액순환을 관찰 할 수 있을 정도로 의 개체 발생 및 기관형성과정이 매우 빠르게 진행되고, 허파를 제외하고는 심장, 간, 췌장, 장등 면역계를 포함한 대부분의 조직기관을 가지고 있다. 또한 Zebrafish의 성체의 크기는 3~4 cm로 작아 사육공간의 제약이 없으며, 암컷은 일주일에 200~300개의 배아를 얻을 수 있다. 이러한 특징들로 인하여 생체 내에서의 세포생물학적 실험이나 대규모 유전학적 연구가 가능하기 때문에 질병연구, 신약개발 발굴의 모델로서의 이용이 용이하다.

질병 중 암은 사망원인별 순위에서 수십년동안 압도적으로 1위를

차지하고 있는 무서운 질병이다. 2014년 통계청에 주요암 사망분율을 살펴보면 사망률이 가장 높은 암종은 폐암(전체 암사망자의 22.8%), 간암 (15.1%), 위암 (11.6%), 대장암 (11.0%), 췌장암 6.7%), 담도암 (5.1%), 유방암 (3.0%), 백혈병 (2.2%), 전립선암 (2.2%), 비호지킨 림프종 (2.1%)의 순을 나타냈다. 암이 걸리는 원인은 아직 분명하게 밝혀지지 않았으나, 국제암 연구소의 통계치에 의하면, 암 발생원인은 식습관 (30%), 흡연 (15~30%), 만성감염 (10~25%), 유전 (5%), 음주 (3%)로 암발생을 야기 시킨다고 발표하였다. 위의 결과에 따르면 암은 식습관에 밀접한 병이므로, 식습관을 조절하면 예방이 가능한 질병이다. 그리고 암을 치료하기 위해 여러 항암제를 사용하고 있으나 이들은 구토, 오열, 설사, 식용부진, 피부염, 발진, 탈모등 심한 부작용이 나타나 여러 문제점을 가지고 있어 여러 부작용이 나타나지 않는 항암제를 개발하는 것은 매우 중요하다.

최근 들어 현대인들의 건강에 대한 관심도가 증가함에 따라 웰빙, 힐링푸드 (Well-being, Healing Food)라 하여 질병을 예방하고 치료하는 음식에 대한 관심이 증가하고 있는 실정이다. 특히 해양생물자원 중 해조류는 식이가 가능하며, 이의 성분으로 다양한 구조와 생리활성도의 특이성을 가지고 있어 현대인의 식탁에서 매우 중요한 음식으로 자리매김

할 가능성이 매우 높다. 또한 해조류가 가지고 있는 다양한 성분으로 질병 예방 및 치료제 개발을 위한 강력한 신물질의 보고로 떠오르고 있다. 청정지역인 제주도는 사면이 바다로 둘러 쌓여 해조류의 보고로 알려져 있으며, 이를 이용한 항암 소재로서의 활용은 사회적 경제 산업적 측면에서 체계적으로 연구할 가치가 있다고 생각된다.

해조류 중 톳은 식이섬유, 칼슘, 철분등이 많이 함유되어있어 소화기능강화, 변비, 빈혈예방, 골다공증에 좋은 식품으로 바다의 불로초로 불리 우고 있다. 최근에는 항고지혈증, 항콜레스테롤, 항응고, 항비만 항당뇨, 항암, 탈모예방등의 톳의 기능성들에 대한 연구가 진행되고 있으며, 톳의 무한한 생리활성 대해서 기대 할 수 있다.

톳의 유용성분을 얻기 위해 시료의 손실을 최소화시키며, 재연성이 확실하고, 단시간의 분리가 가능한 고속원심분배크로마토그래피 (centrifugal partition chromatography, CPC)를 사용하였다.

CPC는 counter-current chromatography(CCC)의 한 분야의 기술로서 용매시스템을 이용하여 물질이 서로 섞이지 않게 2개의 층으로 분리한 뒤 한 층을 이동상으로, 다른 한 층을 고정상으로 하여 고체지지체 없이도 물질을 분리 정제 할 수 있는 시스템이다. 이러한 CPC를 이용하여 one-step과정으로도 순도 높은 물질을 분리해 낼 수 있어 항암물질을

분리해내기 위해 적합하여 CPC를 이용하여 물질을 분리하였다.

따라서 이 연구에서는 Zebrafish에서 암유발 물질과 암세포를 주입하여 암을 유도한 모델을 구축하고, 이 모델을 이용하여 해조류인 툿에서 분리한 saringosterol acetate(SSA)의 항암활성을 확인하였다.

툿은 70% Ethanol로 3시간 동안 3번에 걸쳐 초음파 추출을 하였다. 그 후, 최적의 *n*-hexane : ethylacetate : methanol : water = 5 : 5 : 7 : 1의 비율로 CPC를 이용하여 8개의 fraction을 얻었으며, 그 중 3번 fraction의 ESI/MS와 NMR분석을 통하여 saringostrol acetate를 분리하였다, 이를 Human유래의 간암세포주 (Hep3B cell line), 전립선암세포주 (Du145 cell line)에서 항암활성을 확인하였다. 두개의 세포주에서 SSA는 농도의존적으로 세포를 사멸시켰으며, 샘플을 처리하지 않은 세포(Control)에서 보다 Sub-G1기를 농도의존적으로 늘려주어 세포의 apoptosis을 일으키는 것을 cell cycle을 통하여 확인하였다. 뿐만 아니라 세포성장, 세포생존조절 및 대사, 세포자멸사에 대한 방어에 중요한 역할을 하는 PI3K/Akt/mTOR 기전에서도 SSA는 농도의존적으로 인산화를 억제하는 것을 western blot을 통해 확인하였다.

종양세포가 기저막에 부착되면, 종양 세포에서 분비되는 단백 분해효소에 의해 기저막이 파괴되고 이 파괴된 기저막을 통해 종양 세포가 파급되어

주위의 결합조직으로 전파된다. 또한, 신생혈관생성(angiogenesis)은 종양의 발달, 증식, 전이에 필수적인 과정이다. 따라서 암의 국소침윤과 전이과정에 중요한 역할을 하는 것으로 기저막과 간질의 단백 분해에 중요한 역할을 하는 Matrix metalloproteinase (MMP)와 신생혈관의 생성을 촉진 시키는 Vascular endothelial growth factor (VEGF) 인자들로 종양의 성장과 전이에 대해서 확인을 하였다.

그리고 암에서 발견되는 일부 사이토카인 (Cytokines)은 암에 대한 단순한 숙주의 면역 반응 이외에 신생혈관 형성, 악성종양의 전이 등 생물학적 악성도와 관련이 있는 것으로 알려지면서 염증성 사이토카인 (Inflammatory cytokine)의 중요성이 대두되었다. 암에서 발견되는 대표적 염증성 사이토카인 중에서 다양한 암에서 세포사멸(apoptosis)을 억제하고 암의 성장을 촉진시키며, 암세포의 침윤 및 전이에 중요한 역할을 한다고 알려진 IL-6와 세포를 변형, 증식하며 암을 촉진시킨다고 보고된 TNF- $\alpha$ 의 발현양을 확인하였다. 그리고 상피세포와 조혈세포의 성장, 이동, 분화 및 사멸등을 조절하는 다기능성 사이토카인인 Transformin growth factor- $\beta$  (TGF $\beta$ )을 통하여 신생혈관 형성, 암세포 침윤 및 전이 등 암의 발생과 악성 진행에 대해서 real-time PCR과 Western blot을 통하여 알아보았다. H&E staining을 통하여 조직학적

변이에 대해서도 살펴보았다. 이로써 Zebrafish에 암이 유도 되었는지에 대해서 확인을 하였다.

그 결과 Zebrafish embryos에서 간암을 유도시키는 Diethylnitrosamin (DEN) 물질을 농도별로 처리하였을 때 생존율은 감소하고, ROS (Reactive oxygen species)가 증가, 세포사멸 (Cell death)가 증가하는 것을 확인하였다. 또한 Western blot을 통한 MMP2 and TGF  $\beta$ , real-time PCR을 통한 MMP2, VEGFR2, TGF  $\beta$  가 농도의존적으로 증가하는 것을 확인하여, DEN이 Zebrafish embryos에 간암을 유도하는 것을 확인하였다. 그리고 DEN과 saringosterol acetate을 처리하였을 때에는 위의 지표인자들이 DEN을 처리 하였을 때에는 증가하였으나, saringosterol acetate을 처리하였을 때에는 농도의존적으로 감소하는 것을 확인하였다.

그리고 제브라피쉬 성체에 Human 유래의 Hep3B cell line, Du 145 cell line을 각각 3일에 한번씩 30일 동안  $2 \times 10^6$  cells 과  $5 \times 10^6$  cells을 투여하였을 때 암이 전이 되는지에 대해서 살펴보았다. 그 결과 real-time PCR을 통한 MMP2, VEGFR2, TGF  $\beta$ , IL-6, TNF-  $\alpha$ 가 세포수가 증가할수록 발현 양이 증가하는 것을 확인하였으며, CM-Dil로 염색한 Hep3B, Du145 세포를  $5 \times 10^6$  cells로 투여하였을 때, 간과 장과 배근육에 암세포들이 있는 것을 확하였다. 또한 Western blot을 통한 MMP2, p-

VEGFR2, TGF $\beta$  발현, real-time PCR을 통한 MMP2, VEGFR2, TGF $\beta$ , IL-6, TNF- $\alpha$ , H&E staining을 통한 조직학적 관찰과, 간암 표지자로 알려진 alpha-fetoprotein(AFP), 전립선암 표지자로 알려진 prostate-specific antigen (PSA)을 확인하여 암이 유발됨을 확인하였다. 그리고 saringosterol acetate의 항암활성을 확인하기 위하여 암세포를 투여하기 1주일 전에 saringosterol acetate을 먼저 투여하고 3일에 한번씩 30일 동안 근육 주사하였으며, 암세포 또한 1주일 후 3일에 한번씩 30일 동안 투여하여 항암활성을 확인하였다. 그 결과 saringosterol acetate를 처리하였을 때 Western blot을 통한 MMP2, p-VEGFR2, TGF $\beta$  발현, real-time PCR을 통한 MMP2, VEGFR2, TGF $\beta$ , IL-6, TNF- $\alpha$ , H&E staining을 통한 조직학적 관찰과, 간암 표지자로 알려진 alpha-fetoprotein(AFP), 전립선암 표지자로 알려진 prostate-specific antigen (PSA)에서 농도의존적으로 감소하는 것을 확인 할 수 있었다. 특히 PI3K/Akt/mTOR 경로는 세포성장, 세포생존조절 및 대사, 세포자멸사에 대한 방어에 중요한 역할을 하므로 PI3K/Akt/mTOR 경로를 확인 한 결과 saringosterol acetate가 농도의존적으로 암의 성장과 생존조절을 하는 것을 확인 할 수 있었다.

이 모든 결과를 종합해 볼 때, Zebrafish에서 화학물질 처리와 암세포

주입으로 암이 유도 되는 것을 확인하여 암 모델을 구축하였으며, 이 모델을 이용하여 톳에서 분리한 saringosterol acetate의 항암활성을 확인하였다. 그에 따라 saringosterol acetate는 항암 물질로서 잠재적인 기능성 식품 및 천연의학 소재로서 충분한 가능성이 있으며, Zebrafish 암 모델도 항암 연구에 있어 널리 이용 되어질 것이라 사료 되어진다.

## LIST OF FIGURES

Fig. I . Advantages of zebrafish

Fig. II . The progress of angiogenesis and tumor growth

Fig. III. The photography of a brown alga, *Hizikia Fusiforme*

**Fig. 1-1. TLC analysis of each fraction collected from 70% EtOH extract of *H. fusiforme* by CPC (a), and structure and ESI-MS data of isolated saringosterol acetate (b).** CPC producer: Stationary phase: upper organic phase; mobile phase: lower aqueous phase; flow rate: 2 ml/min; rotation speed: 1000 rpm; sample: 500 mg dissolved in 6 ml mixture of lower phase and upper phase (1:1, v/v) of the solvent system.

**Fig. 1-2. Cytotoxicity of SSA in Hep3B and Du145 cell lines.** Hep3B (A) and Du145 (B) cells ( $5 \times 10^4$  cell/ml) were plated on 24-well plates and treated with SSA at 37°C for 24 h and 48 h. Cytotoxicity of SSA was assessed by lactate dehydrogenase (LDH) assay. Values are expressed as means  $\pm$  S.D. of triplicate experiments. <sup>a-d</sup>Values with different alphabets are significantly different at  $p < 0.05$  as

analyzed by Duncan's multiple range test

**Fig. 1-3. Effect of SSA on cell cycle pattern and apoptosis in Hep3B and Du145 cell lines by flow cytometric analysis.** The Hep3B(A) and Du145(B) cell lines stimulated with 12.5 ~50  $\mu\text{g/ml}$  of SSA and incubated for 48 h. The cells were stained with PI and analyzed by flow cytometry.

**Fig. 1-4. Influence of SSA on PI3K/Akt/mTOR pathway in Hep3B and Du145 cell lines by western blot.** Hep3B(A) and Du145(B) cells ( $5 \times 10^4$  cell/ml) were plated on 6-well plates and treated with SSA at  $37^\circ\text{C}$  for 48 h. Equal amounts of cell lysates (20  $\mu\text{g}$ ) were resolved by SDS-PAGE, transferred to nitrocellulose. <sup>a-d</sup>Values with different alphabets are significantly different at  $p < 0.05$  as analyzed by Duncan's multiple range test.

**Fig. 2-1. Measurement of cancer levels on survival rate (A) and morphology (B) by diethylnitrosamine (DEN) in zebrafish embryos.** The zebrafish embryos were treated with various DEN concentrations at 1 dpf until 3 dpf

**Fig. 2-2. Measurement of cancer levels on ROS production (A) and Cell death (B) with diethylnitrosamine (DEN) treatment in zebrafish embryos.** The zebrafish embryos were treated with various DEN concentrations at 1 dpf until 3 dpf. <sup>a-c</sup>Values with different alphabets are significantly different at  $p < 0.05$  as analyzed by Ducan's multiple range test

**Fig. 2-3. Measurement of cancer levels on proteins expression (MMP2, TGF $\beta$ )(A) and gene expressions (MMP2, VEGFR2, TGF $\beta$ ) (B) by diethylnitrosamine (DEN) in zebrafish embryos.** The zebrafish embryos were treated with various DEN concentrations at 1 dpf until 3 dpf. <sup>a-c</sup>Values with different alphabets are significantly different at  $p < 0.05$  as analyzed by Ducan's multiple range test

**Fig. 2-4. Measurement of toxicity levels on survival rate (A) and cell death (B) by SSA in zebrafish embryos.** The zebrafish embryos were treated with various SSA concentrations at 1 dpf until 3 dpf. <sup>a-c</sup>Values with different alphabets are significantly at different  $p < 0.05$  as analyzed by Ducan's multiple range test.

**Fig. 2-5. Protective effects of SSA on DEN-treated zebrafish embryos; survival**

**rate (A) and morphology (wide type and Tg (fli1:EGFP)) (B).** The zebrafish embryos were exposed to various concentrations of SSA at 1 dpf. After 2 h, a 25  $\mu\text{g/ml}$  of DEN solution was treated to the embryo exposed with SSA for up to 3 dpf. Then, the embryos were rinsed using fresh embryo media.

**Fig. 2-6. Protective effect of SSA on DEN-treated zebrafish embryos; ROS production (A) and Cell death (B).** The zebrafish embryos were exposed to various concentrations of SSA at 1 dpf. After 2 h, a 25  $\mu\text{g/ml}$  DEN solution was treated to the embryo exposed with SSA for up to 3 dpf. Then, the embryos were rinsed using fresh embryo media. <sup>a-c</sup>Values with different alphabets are significantly different at  $p < 0.05$  as analyzed by Duncan's multiple range test.

**Fig. 2-7. Protective effect of SSA on DEN-treated protein expressions (MMP2, TGF $\beta$ )(A) and gene expressions (VEGFR2, MMP2, TGF $\beta$ ) (B) by DEN in zebrafish embryos.** The zebrafish embryos were exposed to various concentrations of SSA at 1 dpf. After 2 h, a 25  $\mu\text{g/ml}$  DEN solution was treated to the embryo exposed with SSA for up to 3 dpf. Then, the embryos were rinsed using fresh embryo media. <sup>a-c</sup>Values with different alphabets are significantly different at  $p < 0.05$  as

analyzed by Duncan's multiple range test

**Fig. 3-1. The mRNA expression levels of VEGFR2, TGF $\beta$ , MMP2, MMP9, TNF- $\alpha$  and IL-6 revealed by rt-PCR in liver tumor xenograft zebrafish liver.** The zebrafish were injected with 20  $\mu$ l of Hep3B cells ( $2 \times 10^6$ ,  $5 \times 10^6$  cells) in to their abdominal cavity once every three days for one month. <sup>a-c</sup>Values with different alphabets are significantly different at  $p < 0.05$  as analyzed by Duncan's multiple range test.

**Fig. 3-2. The mRNA expression levels of VEGFR2, TGF $\beta$ , MMP2, MMP9, TNF- $\alpha$  and IL-6 revealed by rt-PCR in prostate tumor xenograft zebrafish liver.** The zebrafish were injected with 20  $\mu$ l of Du145 cells ( $2 \times 10^6$ ,  $5 \times 10^6$  cells) in to their abdominal cavity once every three days for one month. <sup>a-c</sup>Values with different alphabets are significantly different at  $p < 0.05$  as analyzed by Duncan's multiple range test

**Fig. 3-3. Liver tumor cells showing metastasis and invasion of a 30 dpi zebrafish after xenografted by fluorescent microscopic image.** Hep3B cells were stained

with CM-Dil and injected into the abdominal cavity of zebrafish during ten times a month.

**Fig. 3-4. Prostate tumor cells showing metastasis and invasion of a 30 dpi zebrafish after xenografted by fluorescent microscopic image.** Du145 cells were stained with CM-Dil and injected into the abdominal cavity of zebrafish during ten times a month.

**Fig. 3-5. Measurement of cancer levels on protein expressions (MMP2, TGF $\beta$ , p-VEGFR2)(A), Histological staining (B) and  $\alpha$ -fetoprotein production (C) by liver tumor xenograft zebrafish model** The zebrafish were injected with 20  $\mu$ l of Hep3B ( $5 \times 10^6$  cells) in to their abdominal cavity once every three days for one month. <sup>a-</sup>  
<sup>a</sup>Values with different alphabets are significantly different at  $p < 0.05$  as analyzed by Ducan's multiple range test.

**Fig. 3-6. Measurement of cancer levels on protein expressions (MMP2, TGF $\beta$ , p-VEGFR2)(A), Histological staining (B) and prostate-specific antigen production (C) by prostate tumor xenograft zebrafish model.** The zebrafish were injected

with 20  $\mu$ l of Du145 ( $5 \times 10^6$  cells) in to their abdominal cavity once every three days for one month. <sup>a-c</sup>Values with different alphabets are significantly different at  $p < 0.05$  as analyzed by Ducan's multiple range test.

**Fig. 3-7. The effect of the intramuscular injection of SSA on survival rate (A) and a-fetoprotein production (B) in liver tumor xenograft zebrafish model.** Starting from the day zero the zebrafish were injected with SSA (2  $\mu$ g/g or 5  $\mu$ g/g) once every three days. Starting from the day 7, the zebrafish were injected with 20  $\mu$ l of Hep3B cells ( $5 \times 10^6$  cells) in to their abdominal cavity once every three days for one month. <sup>a-c</sup>Values with different alphabets are significantly different at  $p < 0.05$  as analyzed by Ducan's multiple range test.

**Fig. 3-8. The effect of the intramuscular injection of SSA on Survival rate (A) and prostate-specific antigen production (B) in prostate tumor xenograft zebrafish model.** . Starting from the day zero the zebrafish were injected with SSA (2  $\mu$ g/g or 5  $\mu$ g/g) once every three days. Starting from the day 7, the zebrafish were injected with 20  $\mu$ l of Du145 cells ( $5 \times 10^6$  cells) in to their abdominal cavity once every three days for one month continued with sample treatment. <sup>a-c</sup>Values with different alphabets are

significantly different at  $p < 0.05$  as analyzed by Duncan's multiple range test.

**Fig. 3-9. The effect of SSA on metastasis and invasion in liver tumor xenograft zebrafish model by fluorescent microscopic images.** Starting from the day zero the zebrafish were injected with SSA (2  $\mu\text{g/g}$  or 5  $\mu\text{g/g}$ ) once every three days. Starting from the day 7, the zebrafish were injected with 20  $\mu\text{l}$  of Hep3B cells ( $5 \times 10^6$  cells) in to their abdominal cavity once every three days for one month continued with sample treatment multiple range test.

**Fig. 3-10. The effect of SSA on metastasis and invasion in prostate tumor xenograft zebrafish model by fluorescent microscopic images.** Starting from the day zero the zebrafish were injected with SSA (2  $\mu\text{g/g}$  or 5  $\mu\text{g/g}$ ) once every three days. Starting from the day 7, the zebrafish were injected with 20  $\mu\text{l}$  of Du145 cells ( $5 \times 10^6$  cells) in to their abdominal cavity once every three days for one month continued with sample treatment multiple range test.

**Fig. 3-11. The effect of SSA on H&E (Hematoxylin & Eosin) staining in liver tumor xenograft zebrafish model.** Starting from the day zero the zebrafish were

injected with SSA (2  $\mu\text{g/g}$  or 5  $\mu\text{g/g}$ ) once every three days. Starting from the day 7, the zebrafish were injected with 20  $\mu\text{l}$  of Hep3B cells ( $5 \times 10^6$  cells) in to their abdominal cavity once every three days for one month continued with sample treatment.

**Fig. 3-12. The effect of SSA on H&E (Hematoxylin & Eosin) staining in prostate tumor xenograft zebrafish model.** Starting from the day zero the zebrafish were injected with SSA (2  $\mu\text{g/g}$  or 5  $\mu\text{g/g}$ ) once every three days. Starting from the day 7, the zebrafish were injected with 20  $\mu\text{l}$  of Du145 cells ( $5 \times 10^6$  cells) in to their abdominal cavity once every three days for one month continued with sample treatment.

**Fig. 3-13. The mRNA expression levels of VEGFR2, TGF $\beta$ , MMP2, MMP9, TNF- $\alpha$  and IL-6 revealed by rt-PCR in liver tumor xenograft zebrafish liver.** Starting from the day zero the zebrafish were injected with SSA (2  $\mu\text{g/g}$  or 5  $\mu\text{g/g}$ ) once every three days. Starting from the day 7, the zebrafish were injected with 20  $\mu\text{l}$  of Hep3B cells ( $5 \times 10^6$  cells) in to their abdominal cavity once every three days for one month continued with sample treatment. <sup>a-c</sup>Values with different alphabets are

significantly different at  $p < 0.05$  as analyzed by Duncan's multiple range test .

**Fig. 3-14. The mRNA expression levels of VEGFR2, TGF $\beta$ , MMP2, MMP9, TNF- $\alpha$  and IL-6 revealed by rt-PCR in prostate tumor xenograft zebrafish liver.**

Starting from the day zero the zebrafish were injected with SSA (2  $\mu\text{g/g}$  or 5  $\mu\text{g/g}$ ) once every three days. Starting from the day 7, the zebrafish were injected with 20  $\mu\text{l}$  of Du145 cells ( $5 \times 10^6$  cells) in to their abdominal cavity once every three days for one month continued with sample treatment. <sup>a-c</sup>Values with different alphabets are significantly different at  $p < 0.05$  as analyzed by Duncan's multiple range test .

**Fig. 3-15. The protein expression levels of MMP2, TGF $\beta$  pathway and PI3K/Akt/mTOR pathway revealed by western blot analysis in liver tumor xenograft zebrafish liver.**

Starting from the day zero the zebrafish were injected with SSA (2  $\mu\text{g/g}$  or 5  $\mu\text{g/g}$ ) once every three days. Starting from the day 7, the zebrafish were injected with 20  $\mu\text{l}$  of Hep3B ( $5 \times 10^6$  cells) in to their abdominal cavity once every three days for one month continued with sample treatment. <sup>a-</sup>

<sup>c</sup>Values with different alphabets are significantly different at  $p < 0.05$  as analyzed by Duncan's multiple range test

**Fig. 3-16. The protein expression levels of MMP2, TGF $\beta$  pathway and PI3K/Akt/mTOR pathway revealed by western blot analysis in prostate tumor xenograft zebrafish liver.** Starting from the day zero the zebrafish were injected with SSA (2  $\mu$ g/g or 5  $\mu$ g/g) once every three days. Starting from the day 7, the zebrafish were injected with 20  $\mu$ l of Du145 cells ( $5 \times 10^6$  cells) in to their abdominal cavity once every three days for one month continued with sample treatment. <sup>a-</sup>  
<sup>a</sup>Values with different alphabets are significantly different at  $p < 0.05$  as analyzed by Ducan's multiple range test

**Fig. 3-17. Tumor xenografts in zebrafish embryo. Labeled hepatocellular carcinoma Hep3B cells were injected to transgenic tg(fli1:EGFP) zebrafish embryo at 48 hpf. Then the embryos were analyzed by fluorescence microscopy.** Brightfield image of Hep3B cells inside the tg(fli1:EGFP) transgenic zebrafish embryo at 0 dpi (A). Fluorescence imaging of the embryo at 48 hpi showing interaction between the vasculature (labeled green) and the tumor cells (labeled red) (B).

**Fig. 3-18. Tumor xenografts in zebrafish embryo. Labeled prostate carcinoma Du145 cells were injected to transgenic tg(fli1:EGFP) zebrafish embryo at 48 hpf. Then embryos were analyzed by fluorescence microscopy. Brightfield image of Du145 cells inside the tg(fli1:EGFP) transgenic zebrafish embryo at 0 dpi (A). Fluorescence imaging of the embryo at 48 hpi showing interaction between the vasculature (labeled green) and the tumor cells (labeled red)(B).**

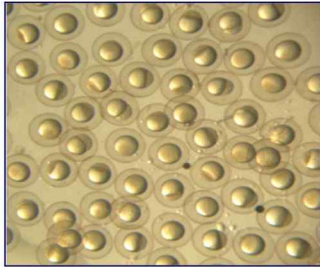
## LIST OF TABLE

**Table 1-1. NMR data for saringosterol acetate in methanol-d<sub>4</sub>**

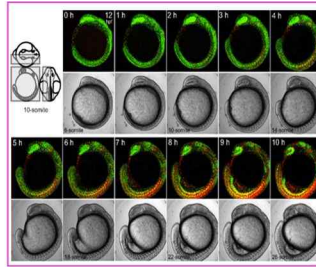
## INTRODUCTION

Zebrafish (*Danio reiro*) were established as a tool for academic developmental biology during 1970s and 1980s owing to their transparent embryos, rapid life cycle and genetical similarity to human. In 1990s, zebrafish were used as the first vertebrate for large scale mutagenesis screening, yielding thousands of mutations, some of which recapitulated human diseases (Hsu et al., 2007). The characteristics features that make zebrafish a popular experimental animal to study the disease mechanisms includes: The embryos are optically transparent so all process of organogenesis may be visualized *in vivo* and investigated in real-time (Eisen, 1996). Organogenesis occurs rapidly, and major organs develops in larvae within 5 to 6 days of post-fertilization (dpf). This enables large scale study for positional cloning as well as diseases characterization due to the fact that females spawn up 200~300 eggs per week. In addition, maintenance costs are significantly lower than those for mammals. And the zebrafish have cardiovascular, nervous, and digestive systems that are similar to those of mammals. Sequencing of the entire genetic composition of the zebrafish has revealed that 70% of protein-coding human genes are concerned with genes found in the zebrafish and that 84% of genes known to be related to human diseases have a zebrafish counterpart (Howe et al, 2013). Thus, the zebrafish

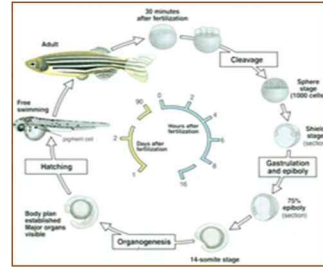
has attracted the attention of scientists engaged in variety of discipline, such as developmental biology, neuroscience, hematopoiesis, nephrological or cardiovascular research owing to the similarities between zebrafish and mammalian biology (Stewart et al., 2014, Jing and Zon, 2011, Chico et al., 2008). Among the diseases, tendency of histopathological and gene expression profiles of zebrafish tumors are similar to that of human. The zebrafish cancer model solves the problems related with murine xenograft models and offers alternative options for studying human tumor angiogenesis and metastasis (Teng et al., 2013). About 50 articles in which zebrafish were used as a cancer model have been published since 2000. Strategies used include carcinogenic treatments, transplantation of mammalian cancer cells, reverse genetic target-selected mutagenesis to inactivate known tumor suppressor genes, forward genetic screens for proliferation or genomic instability, and the generation of transgenics to express human oncogenes. Zebrafish have been found to develop almost any tumor type known from human, with similar morphology, gene expression, and comparable signaling pathways (Feitsma and Cuppen 2008). The most common targeted tissues for neoplasia are the testis, gut, thyroid, liver, peripheral nerve, connective tissue, prostate, and ultimobranchial gland. Less common target tissues includes blood vessels, brain, gill, nasalepithelium, and the



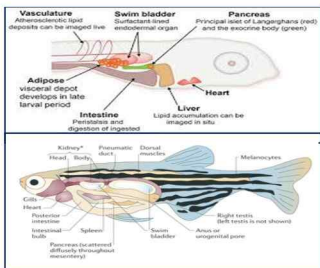
**Large number of offspring  
(200~300 eggs/ wk)**



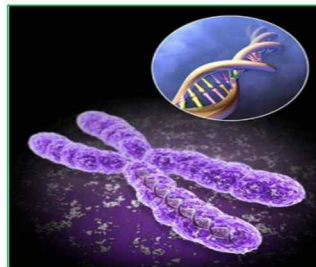
**Small and transparent**



**Fast life cycle**



**Similar organ system  
with human**



**Similar Genes to  
human**



**Small whole length of  
adults : 4 ~ 5 cm**

**Fig. I . Advantages of zebrafish**

Imphomyeloid system (Kent et al., 2002).

Cancer is a dangerous disease in which certain cells in our body grow in an uncontrolled way. It is one of the world's most serious illnesses. The human body has billions of cells. They are tiny elements of living material. Cells always reproduce themselves. However, sometimes due to certain cases cell growth gets out of control and the cell proliferation increases in an abnormal manner. These cells that produce new tissue are called tumors. The most common types of cancer in males are lung cancer, prostate cancer, liver cancer, colorectal cancer, and stomach cancer, and in females, the most common types are breast cancer, colorectal cancer, liver cancer, lung cancer, and cervical cancer. Among the cancer types, prostate cancer is the second-leading cause of cancer-related death in men, which can be estimated as 1 of 6 men in the United States will be diagnosed during their lifetimes. Survival rates are directly associated with early detection, therefore, men are advised to get an annual screening every year. In addition, liver cancer, the most common type of malignant primary liver tumor, considered to be the third most frequent cause of cancer death worldwide.

Cancer has the ability to spread to adjacent or distant organs, which makes it life threatening. Tumor cells can penetrate blood or lymphatic vessels, circulate through

the intravascular stream, and proliferate at another site: collectively known as metastasis (Folkman, 1971). Growth of the vascular network is important for the metastatic spread of cancer tissues. The processes which lead to the formation of new blood and lymphatic vessels are formed through angiogenesis and lymphangiogenesis, respectively (Lockhart et al., 2003). Angiogenesis is a complex process by which new blood vessels are formed from existing vessels; it involves multiple interactions between endothelial cells, surrounding pericytes, and smooth muscle cells, angiogenic cytokines/growth factors. The multiple steps include degradation of the basement membrane surrounding an existing vessel, migration and proliferation of endothelial cells into the new space, maturation, differentiation, and adherence of the endothelial cells to each other, and lumen formation. Angiogenesis can be initiated by the release of proangiogenic factors, vascular endothelial growth factor (VEGF), basic fibroblast growth factor (bFGF), angiogenin, transforming growth factor (TGF)- $\alpha$ , TGF- $\beta$ , tumor necrosis factor (TNF)- $\alpha$ , interleukin-6, hepatocyte growth factor, and epidermal growth factor (Nishida et al., 2006). The VEGF family and their receptors (VEGFR) are receiving an increased attention in the field of neoplastic vascularization. VEGF which is a powerful angiogenic agent in neoplastic tissues. Also endothelial cells activated by VEGF produces matrix

metalloproteinases (MMPs). The MMPs break down the extracellular matrix which formed of protein and polysaccharides and fills the spaces between cells. This matrix permits the migration of endothelial cells.

The endothelial cells begin to divide as they migrate into the surrounding tissues.

TGF- $\beta$  maintains tissue homeostasis and prevents incipient tumors from progressing down the path to malignancy by regulating not only cellular proliferation, differentiation, survival, and adhesion but also the cellular microenvironment. But as genetically unstable entities, cancer cell have the capacity to avoid or worse yet, adulterate the suppressive influence of the TGF- $\beta$  pathway (Massague., 2008).

Moreover, TNF- $\alpha$  can induce such diverse effects as apoptosis, necrosis, angiogenesis, immune cell activation, differentiation, and cell migration. These processes are of great relevance in tumor immune surveillance, and also play crucial roles in tumor development and tumor progression (Wajant. 2009). As well as IL-6 is involved in the host immune defense mechanisms as well as the modulation of growth and differentiation in various malignancies (Guo et al., 2012).

Most of the deaths caused by cancer usually happen after the cells break away from the initial tumor and spread into other sites in the body. Metastasis is the primary cause of human cancer mortality, accounting for >90% of deaths (Spano et al., 2012).

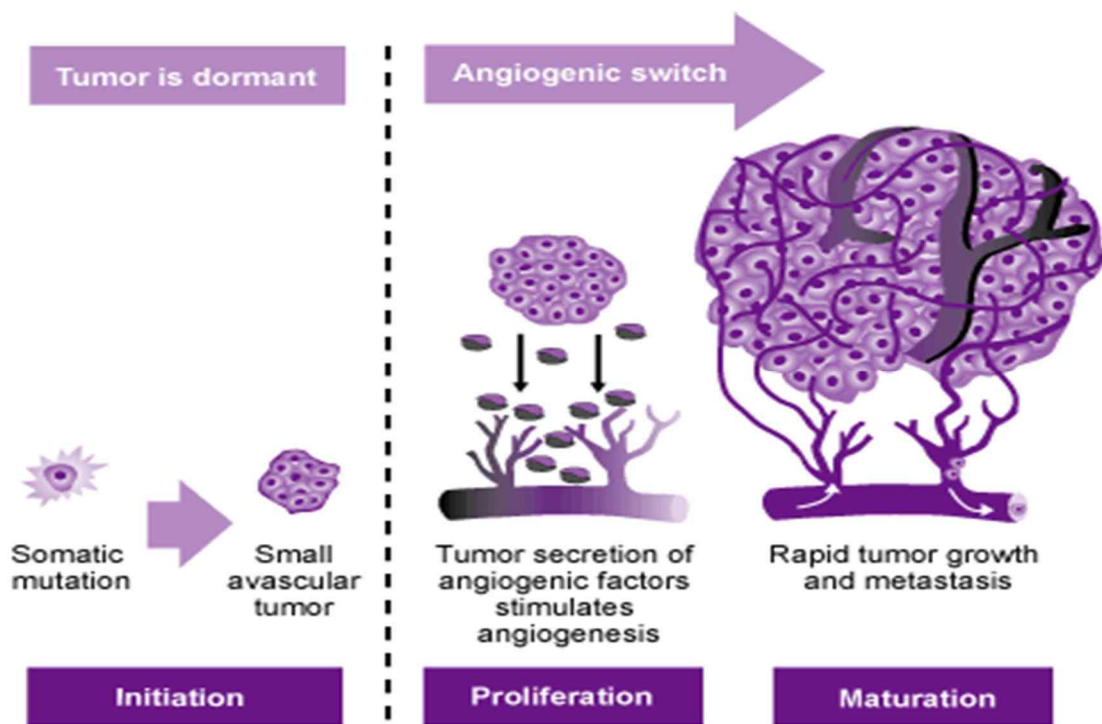


Fig. II. The progress of angiogenesis and tumor growth

Cancer metastasis is a key step of cancer progression that indicates a more advanced stage and a poorer prognosis. Multiple cellular processes, including the degradation of the extracellular matrix (ECM), the epithelial-to-mesenchymal transition (EMT), tumor angiogenesis, the development of an inflammatory tumor microenvironment, and the dysfunction of programmed cell death machinery, have been demonstrated to be essential for cancer metastasis.

Phosphatidylinositol 3-kinase (PI3K/AKT/mammalian target of rapamycin (mTOR)) pathway is involved in many cellular processes including proliferation, differentiation, apoptosis, cell cycle progression, cell motility and tumorigenesis, tumor growth, and angiogenesis

Marine organisms are rich sources of structurally diverse bioactive compounds with valuable nutraceutical, cosmeceutical and pharmaceutical potentials (Barrow and Shahidi, 2008). Among them, marine algae represent one of the richest sources of bioactive secondary metabolites. Seaweeds are distinguished according to the nature of their pigments; brown algae, red algae, and green algae. In Asian countries, several species of seaweed are used as food ingredients and medicine, to provide nutrition and a peculiar taste. Recently, marine algae have been identified as an under-exploited plant resource and functional food (Heo et al., 2005a,b). They have

proven to be a rich sources of structurally diverse bioactive compounds with valuable pharmaceutical and biomedical potential. Among the seaweeds, brown seaweeds have various biological compounds, such as xanthophylls, pigments, fucoidans, phycocolloids, sterol, phlorotannins, and fucoxanthin (Halliwell and Gutteridge, 1999). *Hizkia fusiforme* (class Phaeophyceae, order Fucales, family Sargassaceae), a brown seaweed mainly found, in Korean and Japanese sea has been consumed as a popular food type in both countries (Siriwardhana et al., 2003)(Fig. III.). This alga is known to be rich in dietary fibers, and essential minerals such as calcium, iron and magnesium (Zhu et al., 2010). *H. fusiforme* is not only used as a food product, but also has medical applications and have been suggested to posses antioxidant, anti-coagulant, anticancer, antidiabetic, and antiinflammation effects (Siriwardhana et al, 2003, Kim et al., 1998, Han et al., 2015).

Sterols and related compounds (4a-methyl- and 4,4-dimethyl sterols, ketosteroids, steryl esters and steryl glycosides) are biosynthesized from mevalonic acid via isopentenylpyrophosphate and squalene. Although there is an extensive literature on seaweed sterols, our understanding of their occurrence and distribution is far from complete as a result of all too frequently inadequate identification of isomeric sterol. The predominant sterol of investigated brown algae (some 60 species) is fucosterol



Fig. III. The photography of a brown alga, *Hizikia Fusiforme*

in some cases isomers cholesterol, 24-methylenecholesterol, and 22-dehydrocholesterol are widespread among brown algae; brassicasterol or its 24-S epimer ergosterol, demosterol, stigmasterol, or its 24-R epimer poriferasterol, a C27 cyclopropanoid 'cytosterol', and the probable fucosterol oxidation product saringosterol are less frequently encountered (Komura et al., 1974).

The previous study was reported that the isolated saringosterol acetate derivatives of *H. fusiforme* have anti-cancer activity on A549 cell line. Several studies have reported the advantages of zebrafish as a disease model (Detrich H., 2011). Therefore this study was performed to evaluate the anti-cancer (Liver, Prostate cancer) effects of the saringosterol isolated from *H. fusiforme* and evaluate its possible uses in nutraceutical or functional foods applications to reduce carcinogenic effects on zebrafish cancer induced model. Induction of cancer was achieved using DEN to induced liver cancer in zebrafish embryos. As well as, Hep3B and Du145 cancer xenograft was used to induce tumor growth and metastasis in adult zebrafish.

**Part I .**

**Saringosterol acetate of *Hizikia fusiforme*  
exhibits an anti-cancer effect on Hep3B and  
Du145 cell lines**

## Part I .

### **Saringosterol acetate of *Hizikia fusiforme* exhibits an anti-cancer effect on Hep3B and Du145 cell lines**

#### **1. ABSTRACT**

*Hizikia fusiforme*, an edible brown alga, is widely consumed in Korea, Japan, and China and possesses a number of potentially beneficial biological functionalities, including anti-oxidants, anti-coagulant, anti-cancer, and anti-inflammation. Therefore, the potent anti-cancer effects of saringosterol acetate (SSA) isolated from 70% EtOH extraction of *H. fusiforme* was investigated for its inhibitory effects on liver and prostate cancer in Hep3B and Du145 cell lines. The SSA markedly inhibited cancer cell growth and increased the population of cells in sub-G1 compared to the control. Furthermore, we confirmed that the mechanism involved in this process occurs through PI3K/Akt/mTOR pathway an important regulator of cell growth, metabolism, survival, metastasis, and resistance to chemotherapy. Therefore, SSA significantly reduced the expression of PI3K, Akt, mTOR protein levels in both cells. These results indicated that the SSA has the potential to be used in applications related with

nutraceuticals or functional foods to reduce carcinogenic effects.

## **2. MATERIAL AND METHODS**

### **2.1. Chemicals and reagents**

RPMI 1640 medium, fetal bovine serum (FBS), penicillin-streptomycin and trypsin-EDTA were purchased from Gibco/BRL (Burlington, Ont, Canada). PI was purchased from Sigma-Aldrich (St. Louis, MO, USA). LDH cytotoxicity detection kit was purchased from Promega (Madison, WI, USA).

### **2.2. Preparation of crude extracts from *Hizikia fusiforme***

The dried *H. fusiformis* (600g) was extracted three times with 70% ethanol (EtOH) for 3 h under sonication at room temperature. The extract was concentrated in a rotary vacuum evaporator, and then the concentrated extract was stored in a refrigerator until CPC (centrifugal partition chromatography) separation.

### **2.3. CPC process**

The CPC experiments were carried out using the protocol described by Lee et al (2013). The two phases solvent systems were composed of *n*-hexane:ethylacetate (EtOAc):methanol (MeOH):water = 5:5:7:1. The upper organic phase was used as the mobile phase, and the lower aqueous phase was employed as the stationary phase.

The effluent from the CPC was monitored by TLC analysis with mobile phase composed of  $\text{CHCl}_3$ :MeOH=20:1.

#### **2.4. ESI/MS analysis of purified compound**

ESI/MS analyses were carried out using a Finnigan MAT LCQ ion-trap mass spectrometer (Finnigan MAT, San Jose, CA, USA) equipped with a Finnigan electrospray source and capable of analyzing ions up to  $m/z$  2000. Xcalibur software (Finnigan MAT) was used for the operation. Negative ion mass spectra of the column eluate were recorded in the range  $m/z$  100–2000. The source voltage was set to 4.5 kV and the capillary temperature to  $250^\circ\text{C}$ . The other conditions were as follows: capillary voltage,  $-36.5$  V; inter-octapole lens voltage, 10 V; sheath gas, 80 psi (551.6 kPa); auxiliary gas, 20 psi (137.9 kPa).

#### **2.5. $^1\text{H}$ -NMR and $^{13}\text{C}$ -NMR analysis of purified compound**

$^1\text{H}$ -NMR spectra and  $^{13}\text{C}$ -NMR spectra of the isolated compound was measured with a JEOL JNM-LA 300 spectrometer.

#### **2.6. Cell culture**

The human HCC cell lines Hep3B and human prostate cancer cell line Du 145 were maintained in RPMI supplemented with 10% heat-inactivated FBS, penicillin (100U) and streptomycin (100  $\mu\text{g/ml}$ ). Cultures were maintained at 37°C in 5% CO<sub>2</sub> incubator.

## **2.7. LDH Cytotoxicity assay**

Hep3B and Du145 cells ( $5 \times 10^4$  cells/ml) were plated in 24-well plates and pre-incubated for 16 h and then treated with saringosterol acetate (SSA) at 37°C for 24 h to 48 h. The release of lactate dehydrogenase (LDH) from Hep3B and Du145 cells were used to detect cytotoxicity and was measured at the end of each proliferation experiment. LDH leakage is a means of measuring membrane integrity as a function of the amount of cytoplasmic LDH released from the cytosol into the medium. LDH activity was determined from the production of NADH during the conversion of lactate to pyruvate and was determined using an LDH cytotoxicity detection kit. The culture medium (50  $\mu\text{l}$ ) was transferred into 96-well plate and then incubated with 50  $\mu\text{l}$  of the reaction mixture from the cytotoxicity detection kit for 30 min at room temperature in the dark. 1N HCl (50  $\mu\text{l}$ ) was added to each well to stop the enzymatic reaction. The optical density of the solution was then measured using an

ELISA plate reader at a wavelength of 490 nm.

## **2.8. Cell cycle analysis**

Cell cycle analysis was performed to determine the proportion of apoptotic sub-G<sub>1</sub> hypodiploid cells (Nicoletti et al., 1991). The cells were placed in a 6-well plate at a concentration of  $5 \times 10^4$  cells/ml. Sixteen hours after seeding, the cells were pretreated with the indicated concentration of SSA. After 48h, the cells were harvested at the indicated time and fixed in 1 ml of 70% EtOH for 30 min at 4°C. The cells were washed twice with PBS and incubated in the dark in 1 ml PBS containing 100 µg PI and 100 µg RNase a for 30 min at 37°C. Flow cytometric analysis was performed with a FACS Calibur flow cytometer (Becton Dickinson, San Jose, CA, USA). The effect on cell cycle was determined by the changes in the percentage of cell distribution at each phase of the cell cycle and assessed by histograms generated by the computer program Cell Quest and Mod-Fit.

## **2.9. Western blot analysis**

Cells ( $5 \times 10^4$  cells/ml) in 6-well plate were pretreated with the indicated concentrations of SSA. The cells were lysed in lysis buffer for 10 min and then

centrifuged at 14,000 rpm for 5 min at 4°C. The protein concentrations were determined by using BCA™ protein assay kit. The lysate, which containing 20 µg of protein, was subjected to electrophoresis with a 10% SDS-polycarylamide gel and transferred onto a polyvinylidene fluoride (PVDF) membrane using a glycine transfer buffer (192 mM glycine, 25 mM Tris HCl (pH8.8), 20% methanol (v/v)). The membranes were blocked in a 5% blotting-grade blocker in TBST (a mixture of Tris-buffered saline and Tween 20 used as a buffer for washing nitrocellulose membranes in western blotting) for 2 h. The primary antibodies were washed with TTBT, and then incubated with the secondary antibodies at a 1:3000 dilution. The immunoreactive proteins were detected using an enhanced chemiluminescence (ECL) western blotting detection kit and exposed to Fusion solo..

## **2.10. Statistical analysis**

The data are expressed as the mean± standard error (SE), and one-way ANOVA test (using SPSS ver. 12 statistical software; SPSS Inc., Chicago, IL,USA) was used to compare the mean values of each treatment. Values with different alphabets are significantly different at  $p<0.05$  as analyzed by Duncan's multiple range test.

### 3. RESULTS

#### 3.1. Optimization of two-phase solvent system

Partition coefficients ( $K$ ) for the selection of a suitable two-phase solvent system was the most important determinant for the successful separation of the target samples by the preparative CPC. In order to optimize the most efficient solvent systems to separate target samples, several two-phase solvent ratios were applied with different compositions and volume ratios of the two immiscible solvents that includes *n*-hexane:EtOAc:MeOH:water (v/v), and then their  $K$  values were determined using the size of bands obtained in TLC. The two-phase solvent systems were composed of 5:3:7:1 (*n*-hexane:EtOAc:MeOH:water, v/v) exhibited a band size consistent with the most efficient separation of sterol from *H. fusiforme*.

#### 3.2. Separation of sterol by CPC and its structural identification

The preparative CPC was operated in descending mode (upper phase: stationary phase and lower phase: mobile phase), with 50% retention of the stationary phase in the coil at a pressure of 3.3 MPa at 360 min. The TLC analyzed data of each fraction from preparative CPC is showed in Fig. 1(a). Sterol in fraction 3 reacted with H<sub>2</sub>SO<sub>4</sub> to produce a purple color. After purification of the sterol in fraction 3 by preparative

TLC, the chemical structure of the sterol was analyzed using HPLC-DAD-ESI/MS.  
 $^1\text{H}$ ,  $^{13}\text{C}$ , 2D NMR data and previous reports (shown in table 1) (Permeh et al., 2012).  
The sterol was confirmed as saringosterol acetate with a molecular weight of  $m/z$  469  
(ESI-MS) (Fig. 1 (b)); 11 mg of pure sterol was isolated from 500 mg of the 70%  
EtOH extract with 2.2 % yield.

**Table 1. NMR data for saringosterol acetate in methanol-d4**

Position (C#)	$\delta_C^a$ (ppm)	(mult)	$\delta_H^a$ (mult)
1	37.81	(CH <sub>2</sub> )	1.02/1.29 (m)
2	33.17	(CH <sub>2</sub> )	1.50/1.89 (m)
3	72.56	(CH)	3.87 (m)
4	38.7	(CH <sub>2</sub> )	2.03/2.15 (d/d)
5	143.51	(C)	
6	122.57	(CH)	5.33
7	35.98	(CH <sub>2</sub> )	2.13/1.71
8	37.55	(CH)	1.83
9	51.85	(CH)	1.83
10	41.28	(C)	
11	24.38	(CH <sub>2</sub> )	1.67/1.136
12	43.15	(CH <sub>2</sub> )	1.61/1.02 (m)
13	43.61	(C)	
14	58.31	(CH)	0.94
15	25.46	(CH <sub>2</sub> )	1.27/1.18
16	30.43	(CH <sub>2</sub> )	1.78/1.49
17	57.54	(CH)	0.96 (d)
18	12.48	(CH <sub>3</sub> )	1.29
19	17.19	(CH <sub>3</sub> )	0.88
20	37.03	(CH)	1.07 (d)
21	18.24	(CH <sub>3</sub> )	0.91
22	33.4	(CH <sub>2</sub> )	1.38
23	29.42	(CH <sub>2</sub> )	1.51
24	78.9	(C)	
25	32.43	(CH)	1.63
26	20.03	(CH <sub>3</sub> )	0.72
27	19.52	(CH <sub>3</sub> )	0.72
28	142.35	(CH)	5.79
29	113.64	(CH <sub>2</sub> )	5.10/5.20
Ac	180.72	(C=O)	
	22.33	(CH <sub>3</sub> )	1.89

<sup>a</sup> Multiplicity determined from HSQC-DEPT experiments

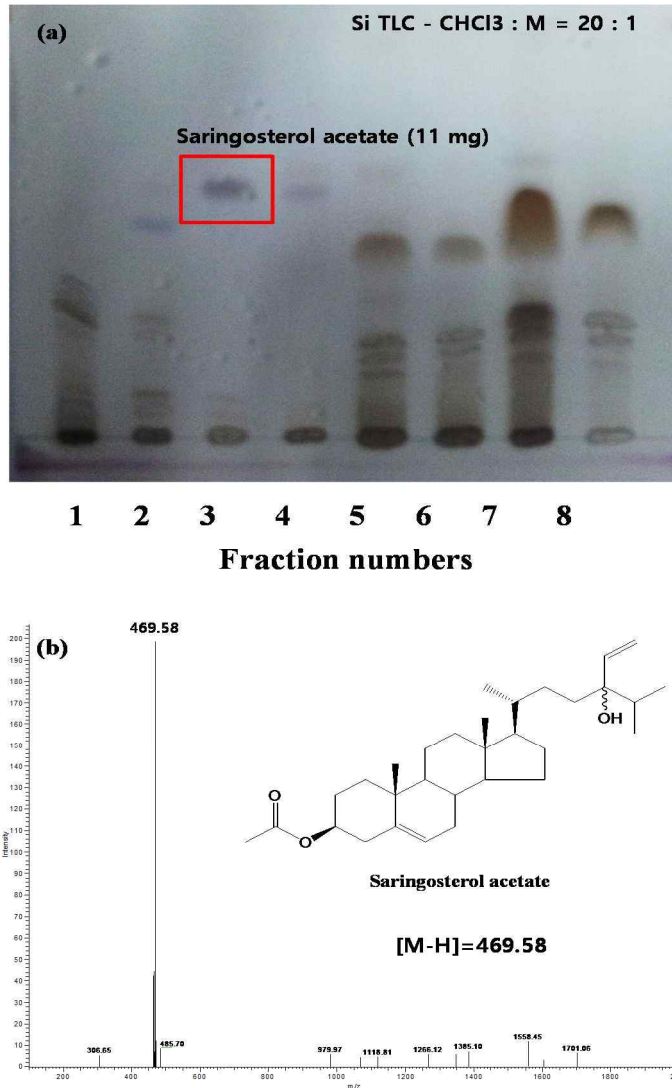


**Fig. 1-1.** TLC analysis of each fraction collected from 70% EtOH extract of *H. fusiforme* by CPC (a), and structure and ESI-MS data of isolated saringosterol acetate (b). CPC producer: Stationary phase: upper organic phase; mobile phase: lower aqueous phase; flow rate: 2 ml/min; rotation speed: 1000 rpm; sample: 500 mg dissolved in 6 ml mixture of lower phase and upper phase (1:1, v/v) of the solvent system.

### **3.3. Cytotoxicity of SSA in Hep3B and Du145 cell lines**

Cytotoxicity of SSA was evaluated using the LDH assay for various concentrations (12.5, 25, 50  $\mu\text{g/ml}$ ) for 24 and 48 h. The half-maximal inhibitory concentration ( $\text{IC}_{50}$ ) was 34.09, 24.50  $\mu\text{g/ml}$  at 48 h in Hep3B and Du145 cells. Thus a dose-dependent reduction in proliferation was observed with the administration of SSA (Fig. 1-2).

### **3.4. SSA induced apoptosis in Hep3B and Du145 cell lines**

Flow cytometric analysis was performed with PI staining as shown in Fig.1-3. When Hep3B and Du145 cells were treated with SSA (12.5, 25, 50  $\mu\text{g/ml}$ ) a dose-dependent increase of the sub-G1 DNA content could be observed with 13.86%, 29.05% and 34.21% increments in Hep3B cell line (Fig.1-3A). Whereas increments of 14.88%, 27.88% and 43.12% could be observed for Du 145 cell line (Fig. 1-3B). In particular, 50  $\mu\text{g/ml}$  of SSA resulted in a significant increase in sub-G1 DNA content. These data show that SSA is able to induce apoptosis in liver and prostate cancer cells.

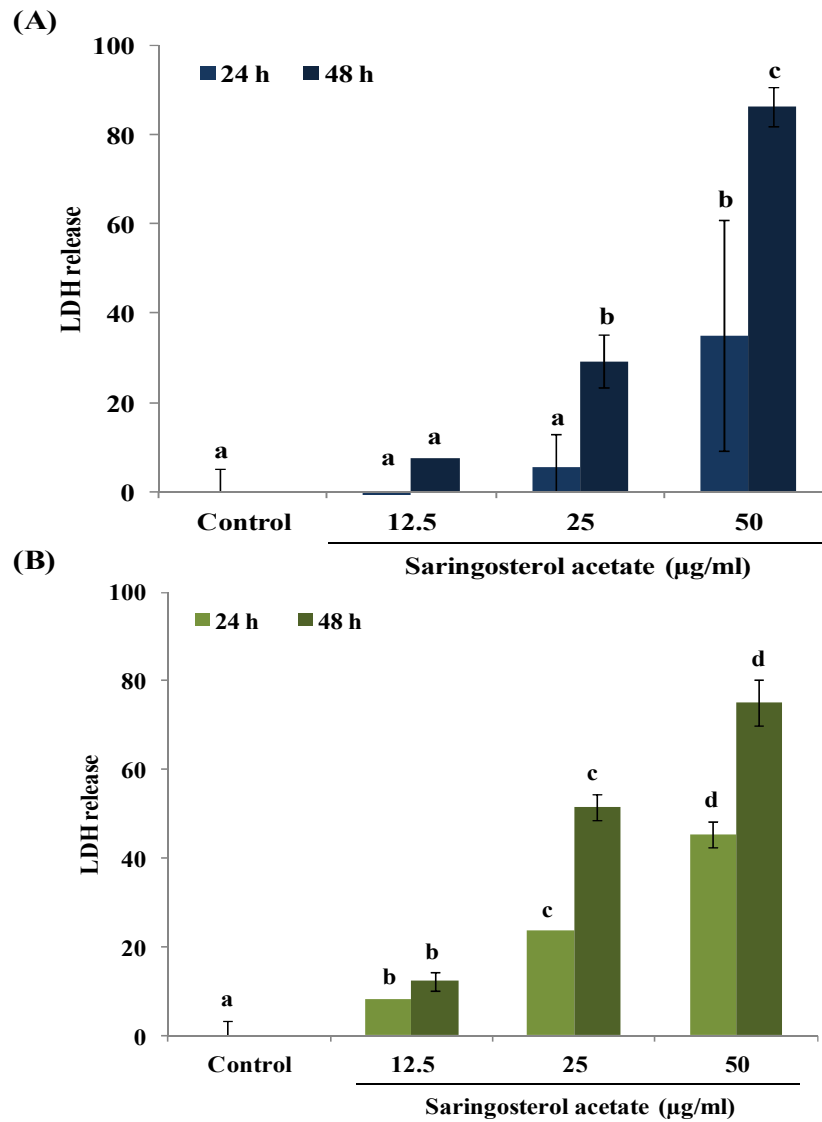


**Fig. 1-2. Cytotoxicity of SSA in Hep3B and Du145 cell lines.** Hep3B (A) and Du145 (B) cells ( $5 \times 10^4$  cell/ml) were plated on 24-well plates and treated with SSA at  $37^\circ\text{C}$  for 24 h and 48 h. Cytotoxicity of SSA was assessed by lactate dehydrogenase (LDH) assay. Values are expressed as means  $\pm$  S.D. of triplicate experiments. <sup>a-d</sup>Values with different alphabets are significantly different at  $p < 0.05$  as analyzed by Duncan's multiple range test.

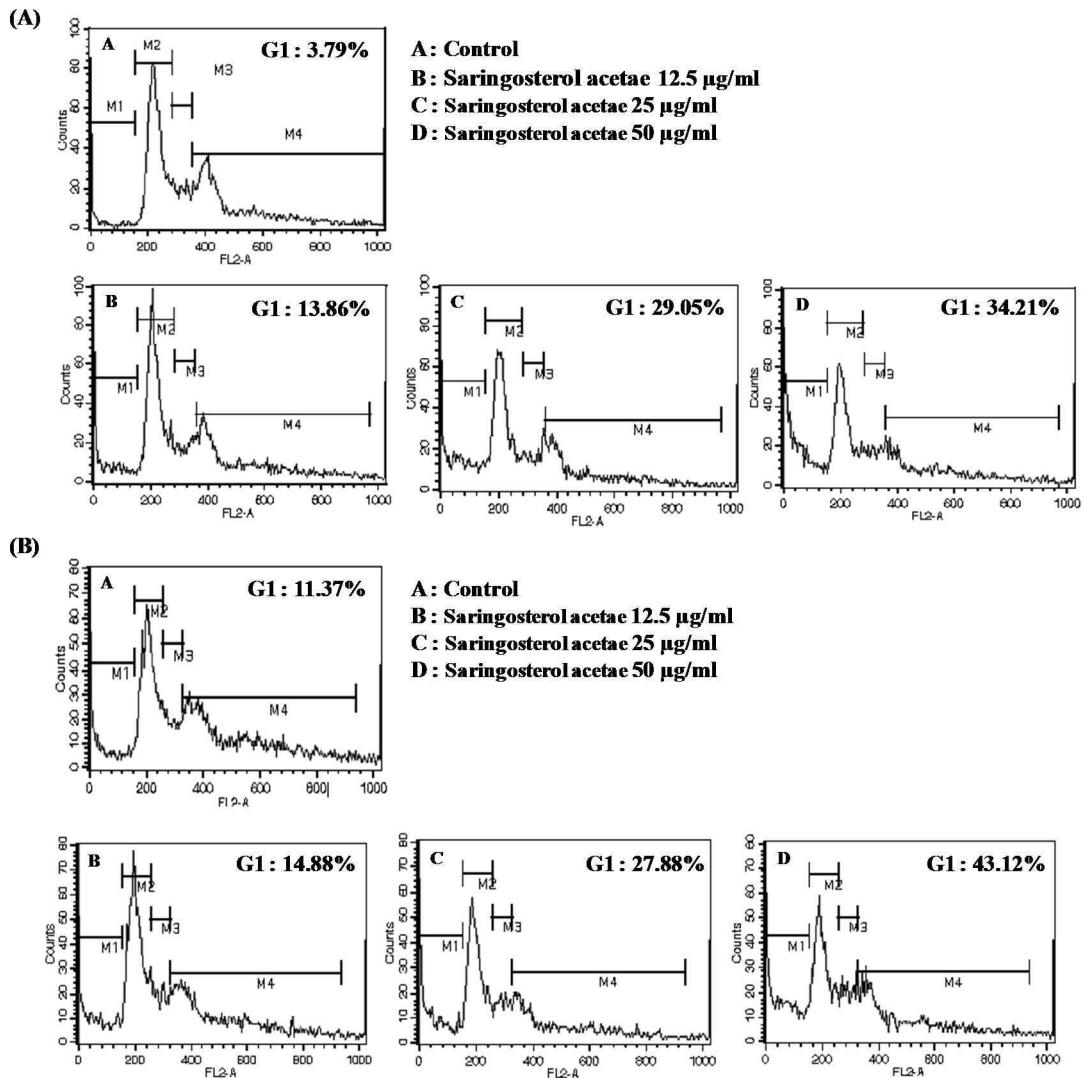


**Fig. 1-3. Effect of SSA on cell cycle pattern and apoptosis in Hep3B and Du145 cell lines by flow cytometric analysis.** The Hep3B(A) and Du145(B) cell lines stimulated with 12.5 ~50 µg/ml of SSA and incubated for 48 h. The cells were stained with PI and analyzed by flow cytometry.

### **3.5. Influence of SSA on PI3K/Akt/mTOR pathway in Hep3B and Du145 cell lines**

PI3K/Akt/mTOR signaling pathway is frequently disturbed in many human cancers. This pathway plays a major role not only in tumor development but also in the tumors potential response to cancer treatment (Vara et al., 2004). We examined the effect of SSA on PI3K/Akt/mTOR pathway in Hep3B and Du145 cells. As shown in Fig. 1-4A, SSA has little effect on PI3K phosphorylation in Hep3B cell line. And SSA treatment significantly inhibited the phosphorylation of Akt in a dose-dependent manner without any effect. Moreover, phosphorylation of mTOR was also inhibited by SSA treatment, which is a downstream protein of Akt. Additionally SSA reduced the phosphorylation of PI3K, Akt, and mTOR proteins in the Du145 cell lines (Fig. 1-4B). In particular, 50  $\mu\text{g/ml}$  of SSA resulted in a significant reduction in expression of the proteins.

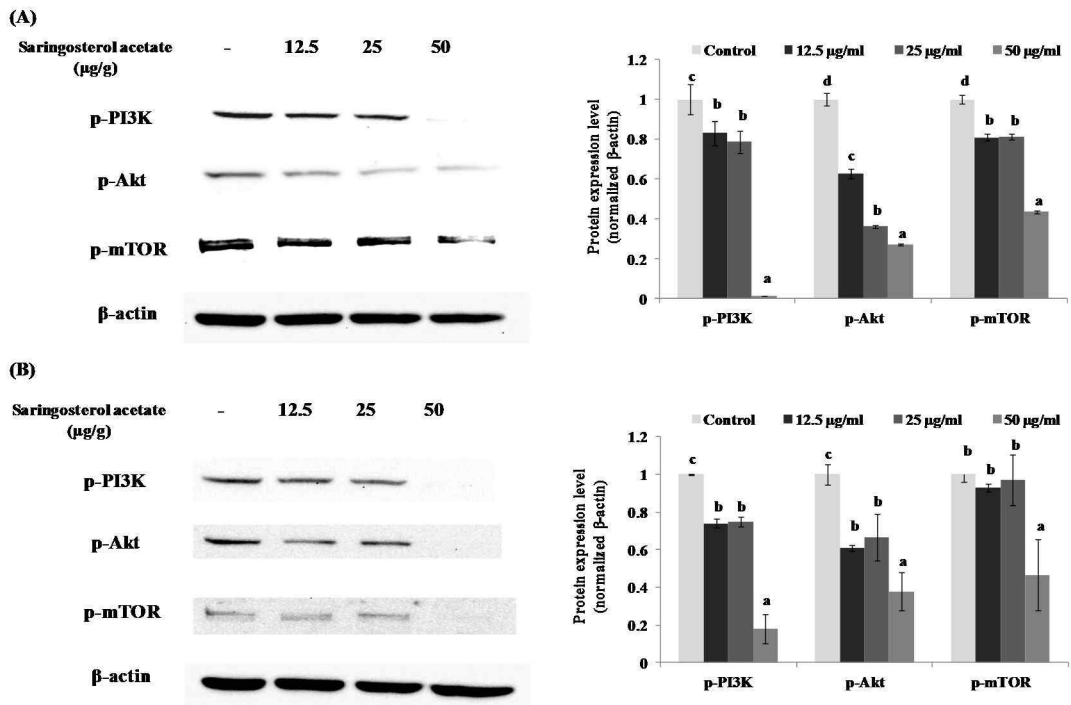


**Fig. 1-4. Influence of SSA on PI3K/Akt/mTOR pathway in Hep3B and Du145 cell lines by western blot.** Hep3B(A) and Du145(B) cells ( $5 \times 10^4$  cell/ml) were plated on 6-well plates and treated with SSA at 37°C for 48 h. Equal amounts of cell lysates (20 μg) were resolved by SDS-PAGE, transferred to nitrocellulose. <sup>a-d</sup>Values with different alphabets are significantly different at  $p < 0.05$  as analyzed by Duncan's multiple range test.

#### 4. DISCUSSIONS

Cancer is a dangerous disease in which certain cells in our body grow in an uncontrolled way. It is one of the world's most serious illnesses. Especially, Prostate cancer is the most common noncutaneous malignancy among men and cause the death of hundreds of thousands of men each year worldwide (Morgans et al., 2015).

Liver cancer is the sixth most commonly diagnosed malignancy and the third leading cause of cancer related mortality, with an estimated 748,000 new cases and 696,000 deaths worldwide in 2008. Patients with intermediate-advanced liver cancer are eligible for palliative treatments including transcatheter arterial chemombolization and the oral multikinase inhibitor, sorafenib. However, treatment benefits are still limited and the development of more effective pharmacological and nutraceutical agents is expected (Jemal et al., 2010).

*H. fusiforme* is not only used as a food product, but also has medical applications and have even been suggested as anti-oxidant, anti-coagulants, anti-cancer antidiabetic, and antiinflammation effects (Siriwardhana et al, 2003, Kim et al., 1998, Han et al., 2009). Therefore, we confirmed that saringosterol acetate, the anti-cancer compound, isolated from *H. fusiforme* have anti-cancer activity on liver and prostate cancer via PI3K/Akt/mTOR pathway. Results from this study indicates that SSA suppresses cell

proliferation in both cell lines (Hep3B and Du145 cell line). And many anti-cancer materials can induce differentiation of tumor cells, arrest cell cycle at the G<sub>0</sub>/G<sub>1</sub> phase, and activate the cell apoptosis gene (Li et al., 2012). SSA significantly increases sub-G<sub>1</sub> DNA contents in cell cycle.

In recent years, it has been shown that PI3K/Akt signaling pathways are involved in the above processes, are frequently disturbed in many human cancer. This pathway plays a major role not only in tumor development but also in the tumor's potential response to cancers. Many of the new "targeted agents" have been specifically designed to act on PI3K/Akt related targets (Vara et al., 2004). These results demonstrate that SSA significantly reduced phosphorylation of PI3K, Akt, and mTOR proteins expression in liver and prostate cancers.

## **5. CONCLUSION**

Overall, our results indicated that SSA could inhibit tumor growth, induce apoptosis and proliferation inhibition by regulating PI3K/Akt/mTOR signaling. Therefore, saringosterol acetate (SSA) isolated from *H. fusiforme* can be used as possible nutraceuticals or functional food to reduce carcinogenic effects.

## **Part II.**

Anti-liver cancer effect of saringosterol acetate in  
diethylnitrosamin-induced zebrafish embryos

## **Part II.**

### **Anti-liver cancer effect of saringosterol acetate in diethylnitrosamin-induced zebrafish embryos**

#### **1. ABSTRACT**

Diethylnitrosamin (DEN) is a well-known potent hepatocarcinogenic agent present in tobacco smoke, water, cured and fried meals, cheddar cheese, agricultural chemicals, cosmetics and pharmaceutical products. DEN is known to induce damage on many enzymes involved in DNA repair and is normally used to induce liver cancer in experimental animal models. Therefore, this study has confirmed an increase in the production of reactive oxygen species (ROS) and induction of cell death by DEN treatment. And angiogenesis is a necessary condition for invasion and metastasis through angiogenic factors (VEGF, TFG $\beta$ 1, MMP2). These factors are also increased by DEN treatment in zebrafish. We observed that exposure to saringostrol acetate (SSA), significantly inhibited DNE induced ROS, cell death and angiogenic factors. These finding indicate that zebrafish model is an efficient animal model that can be used to investigate DEN-stimulated cancer. Therefore, this model can be used as an

*in vivo* experiment to confirm the anticancer properties of functional foods and nutraceuticals

## **2. MATERIAL AND METHODS**

### **2.1. Chemicals and reagents**

DCF-DA (2,7-dichlorodihydrofluorescein diacetate), PI (propidium iodide), and 2-phenoxy ethanol were purchased from Sigma-Aldrich (St. Louis, MO, USA). Antibodies for MMP2, p-VEGFR2 and TGF $\beta$  were obtained from Cell Signaling Technology (Bedford, MA, USA) and  $\beta$ -actin and anti-rabbit secondary antibodies were purchased from Santa Cruz Biotechnology (Santa Cruz, CA, USA). All other chemicals and reagents were of the purest grade available.

### **2.2. Origin and maintenance of parental zebrafish**

Adult zebrafish were obtained from a commercial dealer (Seoul Aquarium, Seoul, Korea) and 15 fish were kept in a 3.5 L acrylic tank under the following conditions:  $28.5 \pm 1$  °C, fed twice a day (Tetra GmgH D-49304 Melle, made in Germany) with a 14/10 h light/dark cycle. Zebrafish were mated and spawning was stimulated by the onset of light. Embryos were then obtained within 30 min of natural spawning and transferred to Petri dishes containing media.

### **2.3. Experimental design of diethylnitrosamin (DEN)-induced cancer**

The embryos (n= 10) were transferred to the individual wells of 12-well plates containing 1.8 mL embryo media. At 7-9 hpf (hour post fertilization), 50  $\mu$ l of various concentration of sample was added to the wells. After 1 dpf (day post fertilization), 50  $\mu$ L of different concentrations of DEN (62.5, 12.5, 25, 50  $\mu$ g/ml) was added to the embryo media, exposing the embryos for up to 3 dpf. The embryos were then rinsed with fresh embryo media.

### **2.4. Determination of ROS production**

Generation of ROS production of zebrafish was analyzed using an oxidation-sensitive fluorescent probe dye, DCFH-DA. At 3 dpf, a zebrafish larva was transferred to one well of 24-well plate, treated with DCFH-DA solution (20  $\mu$ g/mL) and incubated for 1 h in the dark at  $28.5\pm 1$  °C. After the incubation, the zebrafish larvae were rinsed by fresh embryo media and anaesthetized by 0.003% MS-222 (Tricaine methane-sulfonate) before observation and photographed under the microscope CoolSNAP-Pro color digital camera (Olympus, Japan). A fluorescence intensity of individual larva was quantified using the image J program.

## **2.6. Determination of cell death**

Cell death was detected in the live embryos using propidium iodide (PI) staining. PI is membrane impermeable and generally excluded from viable cells. PI is commonly used in identifying dead cells in a population. At 5 dpf, the zebrafish larvae were transferred to one well of a 24-well plate, treated with PI solution (80  $\mu\text{g/ml}$ ), and incubated for 30 min in the dark at  $28.5\pm 1^\circ\text{C}$ . The rest of the procedure was as described in Section 2.5

## **2.7. Real-time PCR analysis**

Embryos collected for RNA isolation ( $n=50\sim 100$ ) were snap frozen in 1.5 ml microcentrifuge tubes using liquid nitrogen and stored at  $-80^\circ\text{C}$ . Total RNA was isolated from embryos using TRIzol (Invitrogen Carlsbad, CA). Total RNA yields were typically 1  $\mu\text{g}/\mu\text{l}$ . Reverse transcription was performed on 1  $\mu\text{g}$  aliquots of total RNA to produce complimentary DNA (cDNA) for real-time reverse transcription-PCR (RT-PCR) (quantitative RT-PCR; qRT-PCR) using an cDNA Synthesis Kit (Roche Diagnostics, Basel, Switzerland). Real-time RT-PCR reactions were performed in triplicate using Roche SYBR Green and cDNA amplification was performed for 45 cycles on a Light Cycler 480 system. Primers to zebrafish  $\beta$ -actin

(forward: 5'-GCCAACAGAGAGAAGATGAC-3', reverse: 5'-CACCAGACTCCATCACAATAC-3'); VEGRF2 (forward: 5'-TGGAGTTCCAGCACCCCTTA-3', reverse: 5'-CGTCCTTCTTCACCCTTTCA -3'); TGFβ1 (forward primer: 5'-CGACTGTAATGCAAACCAGCAGAGCAC-3',reverse: 5'-GTGTCCTCCCATTGAGATGTTATGTATGTC-3'); MMP-2, ( forward primer: 5'-AGCTTTGACGATGACCGCAAATGG -3', reverse: 5'-GCCAATGGCTTGTCTGTTGGTTCT-3').

## 2.8. Western blot analysis

The embryos (n= 50) were transferred to individual wells of 6-well plates containing 2700 ml of embryo media. At 7 to 9 hpf, 150 ml of SSA was added to each of the wells. At 24 hpf, 150 ml of DEN solution was added to each well and these were incubated until 3 dpf. Then, the embryos were rinsed with fresh embryo media. Embryos were transferred into an eppendorf tube, and then washed twice at 5 dpf. The zebrafish were homogenized in lysis buffer using a homogenizer and then centrifuged at 14,000 rpm for 5 min at 4°C. The protein concentrations were determined by using BCA<sup>TM</sup> protein assay kit. The lysate, which containing 30 µg of protein, was subjected to electrophoresis with a 10% SDS-polycarylamide gel and

transferred onto a polyvinylidene fluoride (PVDF) membrane using a glycine transfer buffer (192 mM glycine, 25 mM Tris HCl (pH8.8), 20% methanol (v/v)). The membranes were blocked in a 5% blotting-grade blocker in TBST (a mixture of Tris-buffered saline and Tween 20 used as a buffer for washing nitrocellulose membranes in western blotting) for 2 h. The primary antibodies were washed with TTBT, and then incubated with the secondary antibodies at a 1:3000 dilution. The immunoreactive proteins were detected using an enhanced chemiluminescence (ECL) western blotting detection kit and exposed to Fusion solo.

## **2.9. Statistical analysis**

The data are expressed as the mean $\pm$  standard error (SE), and one-way ANOVA test (using SPSS ver. 12 statistical software; SPSS Inc., Chicago, IL,USA) was used to compare the mean values of each treatment. Values with different alphabets are significantly different at  $p < 0.05$  as analyzed by Duncan's multiple range test.

### 3. RESULTS

#### 3.1. Measurement of cancer levels by DEN in zebrafish embryos

To determine the cancer levels of DEN, we examined the survival rate, morphology, ROS production, cell death, and proangiogenic factors in zebrafish. The survival rate were 96%, 96%, 93%, and 93% in 6.25, 12.5, 25, and 50  $\mu\text{g/ml}$  DNE treated zebrafish at 5 dpf (Fig. 2-1A). The morphology images indicate that yolk sac edema is dose dependent of on the concentrations change the color more dark, respectively at 5 dpf (Fig. 2-1B). And the level of ROS were 132%, 141%, 145% and 159% in 6.25, 12.5, 25, and 50  $\mu\text{g/ml}$  DEN treated groups (Fig2-2A). As shown in Fig. 2-2B, cell death was respectively recorded as 1.2, 1.5, 1.6, and 1.7 fold in 6.25, 12.5, 25, and 50  $\mu\text{g/ml}$  DEN treated groups, compared to the control group. And then angiogenic factors indicated that the phosphorylation of MMP2 and TGF $\beta$  expression is does dependent of concentrations increased by western blot (Fig.2-3A). Besides, mRNA of VEGFR, TGF $\beta$  and MMP2 was significantly increased by DEN treatment (Fig.2-3B). These indicate that DEN imparts cancer effects when administered at high concentration (25  $\mu\text{g/ml}$  and 50  $\mu\text{g/ml}$ ). The DEN concentration of 25  $\mu\text{g/ml}$  was used in subsequent experiments, owing to the higher ROS generation and angiogenic factors observed using 50  $\mu\text{g/ml}$  of DEN

### **3.2. Embryo toxicity of Saringosterol acetate (SSA)**

To determine the toxicity of SSA, we examined the survival rate and cell death in zebrafish embryo. Survival rate was 100% in the all the concentrations (6.25, 12.5, 25, 50  $\mu\text{g/ml}$ ) of SSA compared to the control. But SSA show that cell death was recorded as 1.04, 1.06, 1.18, and 1.31 fold in 6.25, 12.5, 25, and 50  $\mu\text{g/ml}$ . These indicate that SSA imparts little toxicity when administered at high concentration (25  $\mu\text{g/ml}$  and 50  $\mu\text{g/ml}$ ). Therefore SSA concentration of 12.5  $\mu\text{g/ml}$  or lower than that were used in subsequent experiments.

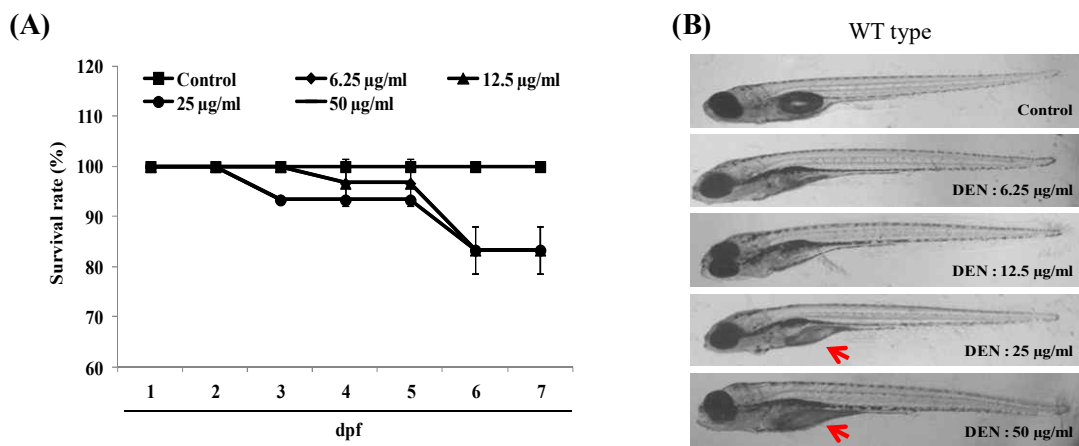


**Fig. 2-1. Measurement of cancer levels on survival rate (A) and morphology (B) by diethylnitrosamine (DEN) in zebrafish embryos.** The zebrafish embryos were treated with various DEN concentrations at 1 dpf until 3 dpf

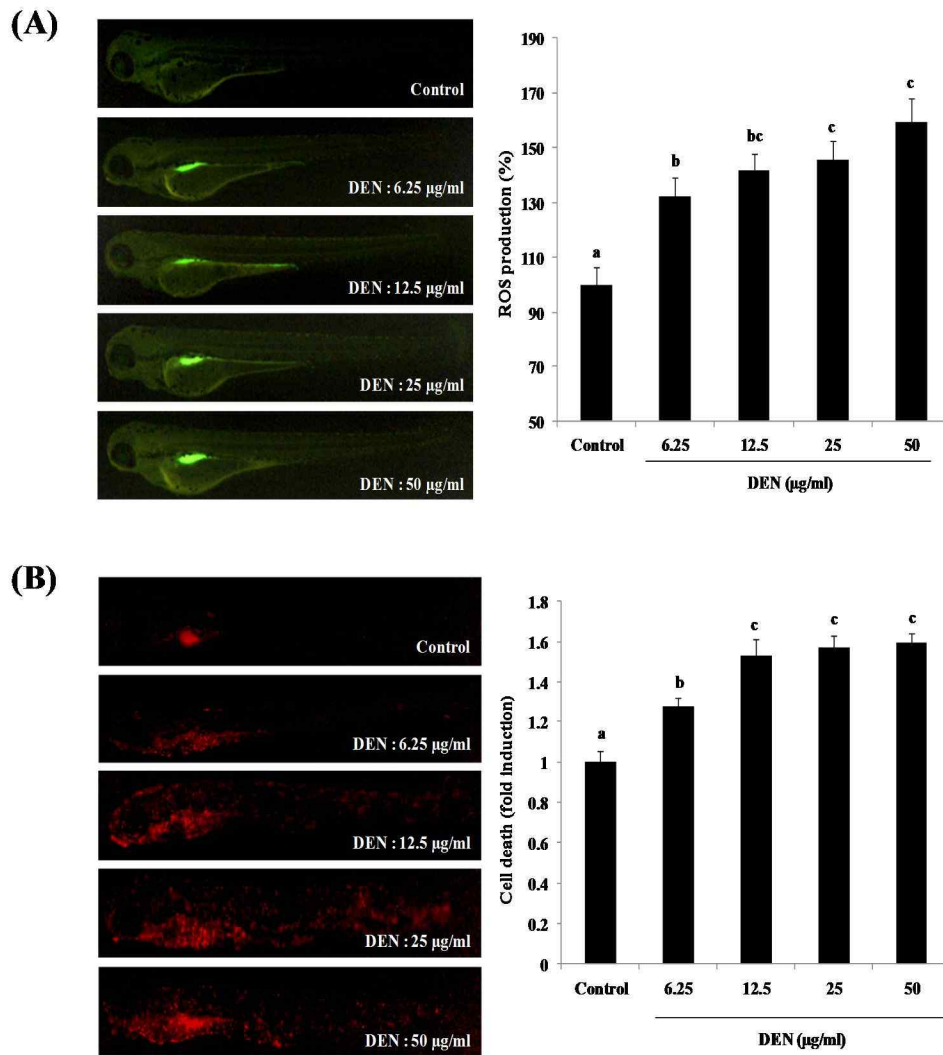


**Fig. 2-2. Measurement of cancer levels on ROS production (A) and Cell death (B) with diethylnitrosamine (DEN) treatment in zebrafish embryos.** The zebrafish embryos were treated with various DEN concentrations at 1 dpf until 3 dpf. <sup>a-c</sup>Values with different alphabets are significantly different at  $p < 0.05$  as analyzed by Ducan's multiple range test

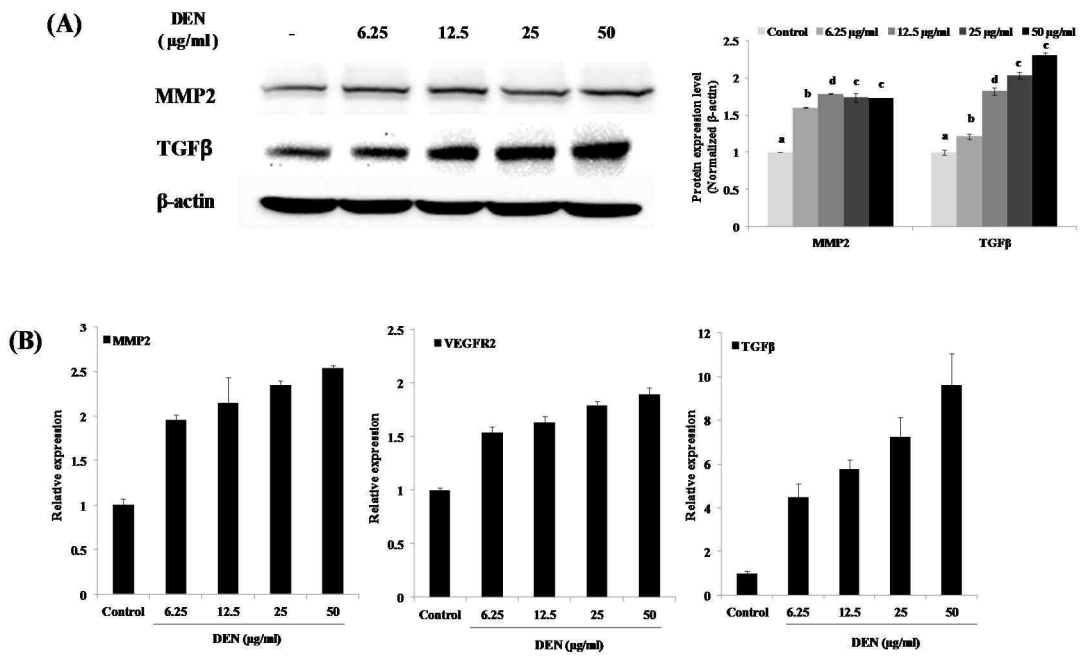
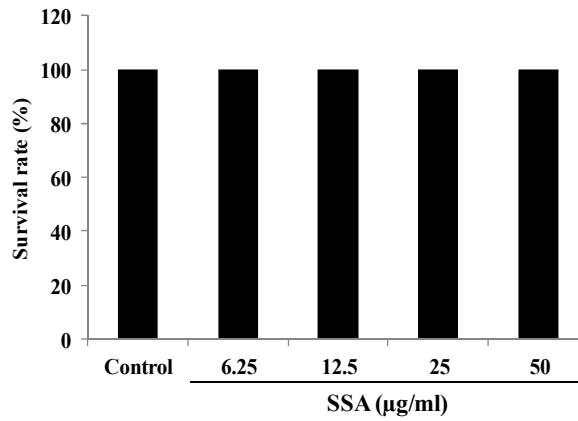


**Fig. 2-3. Measurement of cancer levels on proteins expression (MMP2, TGFβ)(A) and gene expressions (MMP2, VEGFR2, TGFβ) (B) by diethylnitrosamine (DEN) in zebrafish embryos. The zebrafish embryos were treated with various DEN concentrations at 1 dpf until 3 dpf. <sup>a-c</sup>Values with different alphabets are significantly different at  $p < 0.05$  as analyzed by Ducan's multiple range test**

(A)



(B)

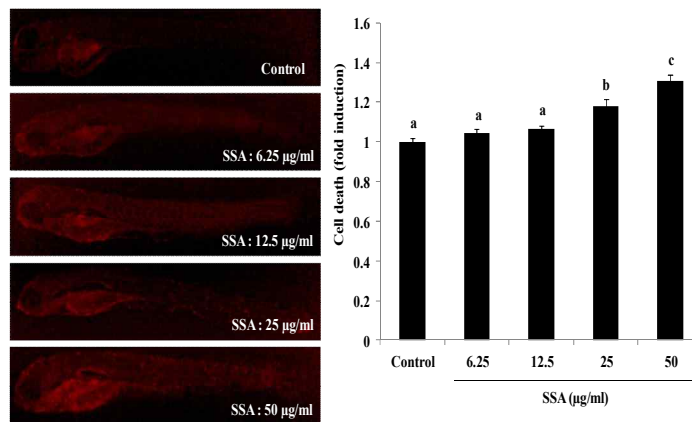


**Fig. 2-4. Measurement of toxicity levels on survival rate (A) and cell death (B)**

**by SSA in zebrafish embryos.** The zebrafish embryos were treated with various SSA concentrations at 1 dpf until 3 dpf. <sup>a-c</sup>Values with different alphabets are significantly at different  $p < 0.05$  as analyzed by Duncan's multiple range test.

### 3.3. Protective effect of SSA against DEN-induced cancer in zebrafish embryo

To confirm the reduction in cancer by SAA, we monitored the survival rate, morphology (wide type and transgenic type (fli1;EGFP)), cell death as well as angiogenic factors by protein and mRNA expression. The survival rates of zebrafish treated with 25  $\mu\text{g/ml}$  DEN or co-treated with SSA are presented in Fig. 2-5A. The survival rate was 95% in the DEN-treated zebrafish. However, the survival rates increased to 100% in the SSA-treated zebrafish of all concentrations (3.13, 6.25, 12.5  $\mu\text{g/ml}$ ). And the morphology images indicates that yolk sac edema is dose dependent of the concentration changes whereas the color became more dark, respectively at 5 dpf. As shown in Fig.2-5B, The morphology images suggests that yolk sac edema of DEN-treated is more darker than SSA-treated zebrafish. The vascularization was observed to be a reduced level in DEN-treated group compared to the control. But SSA-treated zebrafish were having more thick vascularization than DEN-treated zebrafish in transgenic type zebrafish (Fli1:EGFP). The level of ROS was 151% in DEN-treated zebrafish compared to the control. In contrast, the levels of ROS were 149%, 131%, and 119% in the SSA-treated groups (3.13, 6.25, 12.5  $\mu\text{g/ml}$ ), respectively (Fig. 2-6A). SSA treatment of the zebrafish significantly inhibited DEN-induced ROS production. The DEN induced in zebrafish were 1.6 fold, compared to

control. However, treatment with SSA significantly reduced the cell death to 1.10, 1.03, 1.02 fold (Fig. 2-6B). And then angiogenic factors indicate that phosphorylation of MMP2 and TGF $\beta$  expression increase in DEN-treated group. But the treatments with SSA significantly reduced the proteins expression in a dose-dependent manor (Fig. 2-7A). Finally, mRNA of VEGFR, TGF $\beta$  and MMP2 were induced by DEN treatment, and SSA markedly reduced the expression of these genes (Fig. 2-7B)

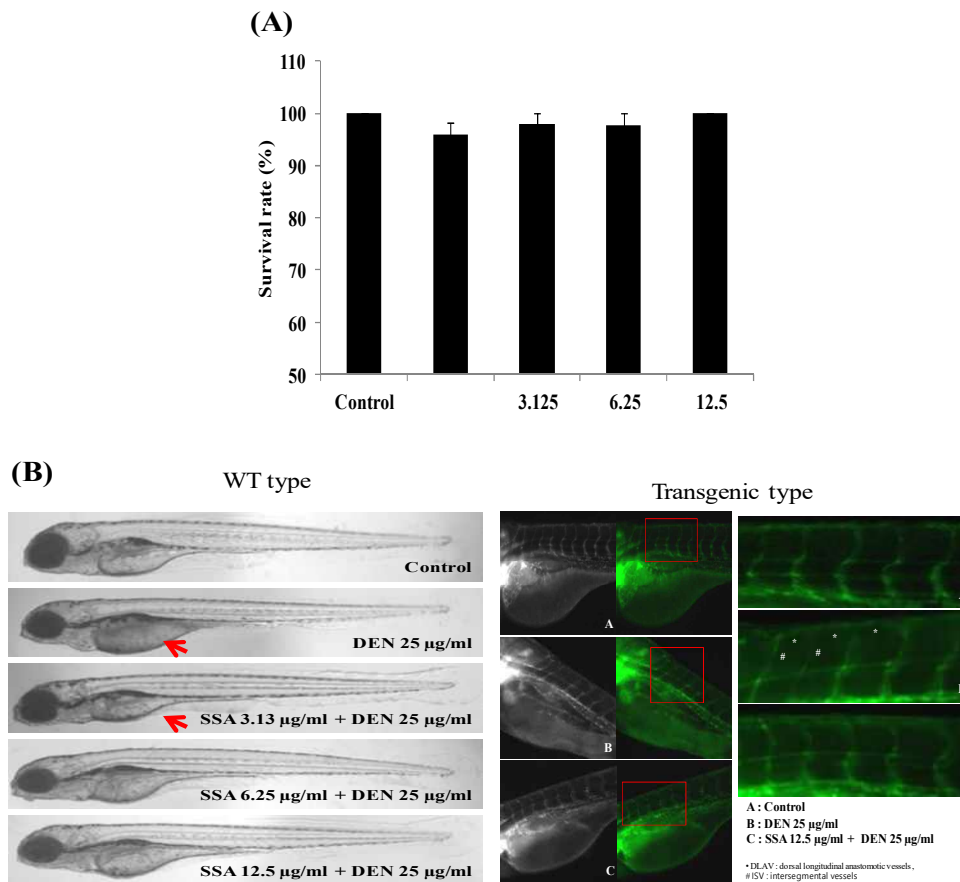


**Fig. 2-5. Protective effects of SSA on DEN-treated zebrafish embryos; survival rate (A) and morphology (wide type and Tg (fli1:EGFP)) (B).** The zebrafish embryos were exposed to various concentrations of SSA at 1 dpf. After 2 h, a 25 µg/ml of DEN solution was treated to the embryo exposed with SSA for up to 3 dpf. Then, the embryos were rinsed using fresh embryo media.

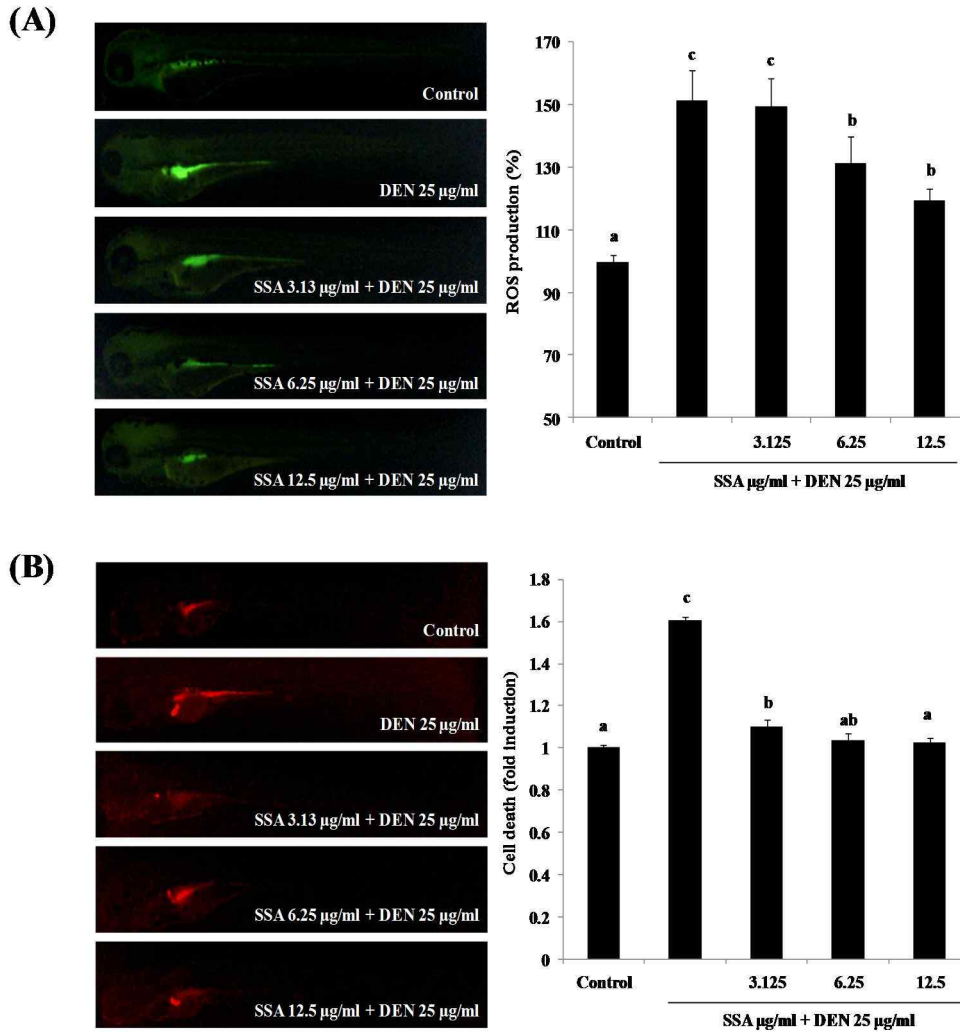


**Fig. 2-6. Protective effect of SSA on DEN-treated zebrafish embryos; ROS production (A) and Cell death (B).** The zebrafish embryos were exposed to various concentrations of SSA at 1 dpf. After 2 h, a 25 µg/ml DEN solution was treated to the embryo exposed with SSA for up to 3 dpf. Then, the embryos were rinsed using fresh embryo media. <sup>a-c</sup>Values with different alphabets are significantly different at  $p < 0.05$  as analyzed by Duncan's multiple range test.

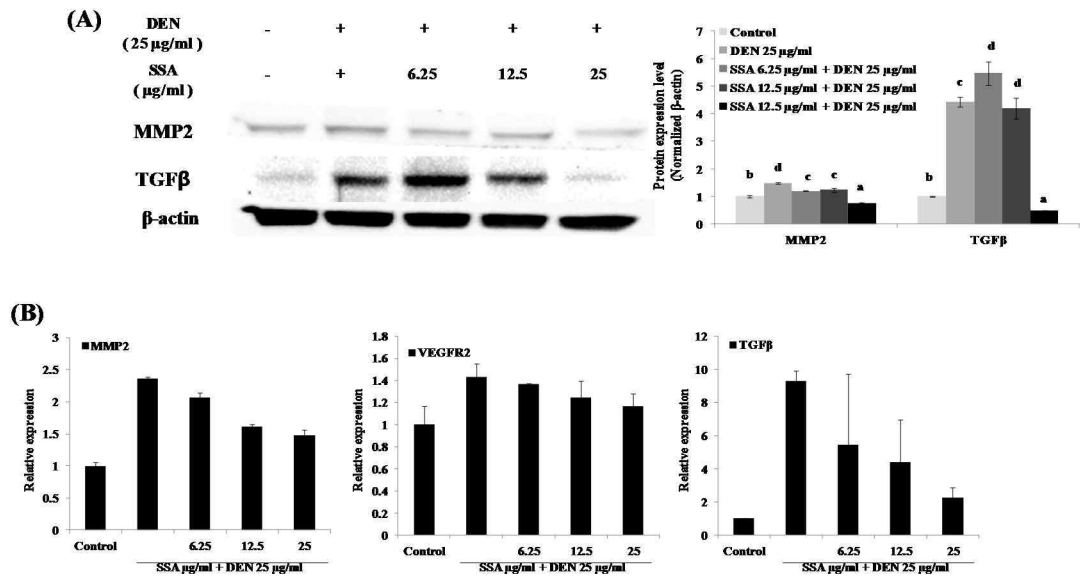


**Fig. 2-7. Protective effect of SSA on DEN-treated protein expressions (MMP2, TGFβ)(A) and gene expressions (VEGFR2, MMP2, TGFβ) (B) by DEN in zebrafish embryos.** The zebrafish embryos were exposed to various concentrations of SSA at 1 dpf. After 2 h, a 25 µg/ml DEN solution was treated to the embryo exposed with SSA for up to 3 dpf. Then, the embryos were rinsed using fresh embryo media. <sup>a-c</sup>Values with different alphabets are significantly different at  $p < 0.05$  as analyzed by Duncan's multiple range test

#### 4. DISCUSSION

The zebrafish has emerged as a popular model species in various fields of research. It has various advantages such as the rapid development of embryo and optical transparency. Further, the zebrafish is similar to mammals in terms of its genetics, physiology, anatomical structure and immune functions. Accordingly, the zebrafish has been increasingly used in biomedical research studies (Lan et al., 2009; Gleeson et al., 2007).

Angiogenesis is the process of generating new capillary blood vessels. It plays an important role in the proliferation, invasion, and metastasis of malignant tumors. It is regulated by the production of angiogenic stimulators including VEGF, TGF $\beta$  and MMP2. VEGF is a key regulatory factor in the prognosis of various cancers (El-Aarag et al., 2014). The TGF $\beta$  signaling pathway is a key player in metazoan biology, and its miss regulation can result in tumor development. The regulatory cytokine TGF $\beta$  exerts tumor-suppressive effects that cancer cell must elude for malignant evolution (Massague, 2008). MMPs are a family of enzymes that proteolytically degrade various components of the MMPs. High expression levels of certain MMPs, either by the tumor cells themselves or by infiltrating inflammatory cells, are closely correlated with tumor invasion and metastatic potential. Especially, MMP2 and

MMP9 have been shown to play critical roles in the “angiogenic switch” and tumor cells could synthesize and secrete large amounts of MMP2 and MMP in a paracrine and/or autocrine manner to stimulate angiogenesis and to increase VEGF release (Zheng et al., 2006). We confirmed that the vascularisation was lower in DEN-treated group compared to the control. But SSA-treated zebrafish indicated much thicker vascularization than DEN-treated zebrafish in transgenic type zebrafish (Flil:EGFP) (Fig.2-3). And we confirmed a significant increase of angiogenic factors in DEN-treated (Fig. 2-3). We determined the protective effects of SSA against DEN-induced cancer through angiogenic factors (Fig.2-7). Our results suggest that SSA could inhibit angiogenesis by down-regulating VEGFR2, TGF $\beta$  and MMP2 expression in zebrafish embryos.

## **5. CONCLUSION**

These findings suggest that the zebrafish model is an efficient animal model that can be used to investigate DEN-stimulated cancer. Therefore, this model can be used as an *in vivo* experiment to confirm the anticancer properties of functional food and nutraceuticals

### **Part III.**

The potential anti-metastatic and anti-invasive effects of saringosterol acetate of *Hizikia fusiforme* in liver and prostate tumor xenograft zebrafish model

## **Part III.**

# **The potential anti-metastatic and anti-invasive effects of saringosterol acetate of *Hizikia fusiforme* in liver and prostate tumor xenograft zebrafish models**

### **1. ABSTRACT**

The zebrafish model system is one of the most widely used animal models. That is attaining popularity as becomes an attractive model for molecular genetics, developmental biology, drug discovery and screening of human disease. Especially, the adult zebrafish has the potential to become an impact model for cancer-related research. Metastasis is a key step of cancer progression that indicates a more advanced stage and a poorer prognosis. Therefore, in this study, we established that anti-metastatic and anti-invasive effects were occurred in cancer xenograft zebrafish model. The zebrafish were injected with 20  $\mu$ l of Hep3B or Du 145 cells ( $2 \times 10^6$  or  $5 \times 10^6$  cells) in to their abdominal cavity once every three days for one month. After one month, angiogenic factors (VEGF, TGF $\beta$ , MMP2, MMP9, IL6, and TNF- $\alpha$ ) were significantly increased in HepB and Du145-injected zebrafish models. And

liver factor,  $\alpha$ -fetoprotein (AFP), was higher than normal group. Also, prostate factor, prostate-specific antigen (PSA), increased dose-dependently with cancer cell concentrations. Therefore, a cell count of  $5 \times 10^6$  was used in subsequent experiment. Then, we confirmed that saringosterol acetate (SSA) isolated from *Hizikia fusiforme* have anti-metastatic and anti-invasive activities in cancer cell xenograft zebrafish model. The zebrafish were injected with SSA (2  $\mu\text{g/g}$  or 5  $\mu\text{g/g}$ ) once every three days. After a week, the abdominal cavity of zebrafish were inoculated with 20  $\mu\text{l}$  of Hep3B or Du145 cells ( $5 \times 10^6$  cells) during ten times a month. All angiogenic factors, AFP, PSA significantly reduced compared to cancer cell injected groups. We observed a decreased expression of MMP2 and TGF $\beta$  pathways and phosphorylation of PI3k/Akt/mTOR pathways in the liver tissues treated with SSA at 5  $\mu\text{g/g}$  concentration. Therefore, this model can be used as an *in vivo* experiment to confirm the anti-metastatic and anti-invasive effects of cancer.

## **2. MATERIAL AND METHODS**

### **2.1. Chemicals and reagents**

RPMI 1640 medium, fetal bovine serum (FBS), penicillin-streptomycin and trypsin-EDTA were purchased from Gibco/BRL (Burlington, Ont, Canada). fluorescent cell tracker CM-Dil was purchased from Invitrogen (Blijswijk, Netherlands)

### **2.2. Cell culture**

The human HCC cell lines Hep3B and human prostate cancer cell line Du 145 were maintained in RPMI supplemented with 10% heat-inactivated FBS, penicillin (100U) and streptomycin (100 µg/ml). Cultures were maintained at 37°C in 5% CO<sub>2</sub> incubator.

### **2.3. Fluorescent cell labeling**

Non-fluorescent cells were labeled with the fluorescent cell tracker CM-Dil (Invitrogen, Blijswijk, Netherlands) according to the manufacturer's instructions.

Briefly, the cells were grown in a 60 nm dish, and transferred to 1.5 ml eppendorf tubes and centrifuged 5 min, at 1,200 rpm. Cells were re-suspended in PBS containing CM-Dil (4 ng/µl final concentration). Cells stained with CM-Dil were

incubated for 4 minutes at 37°C and then 15 minutes at 4°C. After this period cells were centrifuged for 5 minutes at 1,200 rpm, the supernatant discarded and cells re-suspended in media, centrifuged again and washed two times with PBS. Cells were suspended in PBS for injection into the zebrafish.

#### **2.4. Origin and maintenance of parental zebrafish**

Adult zebrafish were obtained from a commercial dealer (Seoul Aquarium, Seoul, Korea) and 15 fish were kept in a 3.5 L acrylic tank under the following conditions: 28.5 ± 1°C, fed twice a day (Tetra GmgH D-49304 Melle, made in Germany) with a 14/10 h light/dark cycle. Zebrafish were mated and spawning was stimulated by the onset of light. Embryos were then obtained within 30 min of natural spawning and transferred to petri dishes containing media.

#### **2.5. Experimental design of liver cancer cell xenograft**

The zebrafish were injected with SSA (2 µg/g or 5 µg/g) once every three days. After a week, the zebrafish abdominal cavity of the zebrafish were injected with 20 µl of Hep3B and Du145 cells (5x10<sup>6</sup> cells) during ten times a month.

## **2.6. Determination of $\alpha$ -fetoprotein(AFP) production and prostate-specific antigen(PSA) production**

Zebrafish blood were subsequently employed for the AFP and PSA measuring using one step AFP ELISA and one step PSA ELISA kit (Diakey).

## **2.7. Real-time PCR analysis**

Zebrafish liver collected for RNA isolation were snap frozen in 1.5 ml microcentrifuge tubes using liquid nitrogen and stored at  $-80^{\circ}\text{C}$ . Total RNA was isolated from embryos using TRIzol (Invitrogen Carlsbad, CA. Total RNA yields were typically  $1\ \mu\text{g}/\mu\text{l}$ . Reverse transcription was performed on  $1\ \mu\text{g}$  aliquots of total RNA to produce complimentary DNA (cDNA) for real-time reverse transcription-PCR (RT-PCR) (quantitative RT-PCR; qRT-PCR) using an cDNA Synthesis Kit (Roche Diagnostics, Basel, Switzerland). Real-time RT-PCR reactions were performed in triplicate using Roche SYBR Green and cDNA amplification was performed for 45 cycles on a LightCycler 480 system. Primers to zebrafish  $\beta$ -actin (forward: 5'-GCCAACAGAGAGAAGATGAC-3', reverse: 5'-CACCAGACTCCATCACAATAC-3'); VEGRF2 (forward: 5'-TGGAGTTCCAGCACCTTA-3', reverse: 5'-CGTCCTTCTTCACCCTTTCA -3');

TGFβ1 (forward primer: 5'-CGACTGTAATGCAAACCAGCAGAGCAC-3',reverse: 5'-GTGTCCTCCCATTGAGATGTTATGTATGTC-3'); MMP-2, ( forward primer: 5'-AGCTTTGACGATGACCGCAAATGG -3', reverse: 5'-GCCAATGGCTTGTCTGTTGGTTCT-3'); MMP-9, (forward primer: 5'-AACCACCGCAGACTATGACAAGGA -3',reverse: 5'-GTGCTTCATTGCTGTTCCCGTCAA-3'); IL-6 ( forward primer: 5'-TCAACTTCTCCAGCGTGATG-3',reverse: 5'-TCTTTCCTCTTTTCCTCCTG-3'); TNF-α (forward primer: 5'-TAGAACAACCCAGCAAAC-3',reverse: 5'-ACCAGCGGTAAAGGCAAC-3').

## 2.8. Western blot analysis

The zebrafish liver tissues were homogenized in lysis buffer using a homogenizer and then centrifuged at 14,000 rpm for 5 min at 4 °C. The protein concentrations were determined by using BCA<sup>TM</sup> protein assay kit. The lysate, containing 30 μg of protein, was subjected to electrophoresis with a 10% SDS-polycarylamide gel and transferred onto a polyvinylidene fluoride (PVDF) membrane using a glycine transfer buffer (192 mM glycine, 25 mM Tris HCl (pH8.8), 20% methanol (v/v)). The membranes were blocked in a 5% blotting-grade blocker in TBST (a mixture of

Tris-buffered saline and Tween 20 was used as a buffer for washing nitrocellulose membranes in western blotting) for 2 h. The primary antibodies were washed with TTBT, and then incubated with the secondary antibodies at a 1:3000 dilution. The immunoreactive proteins were detected using an enhanced chemiluminescence (ECL) western blotting detection kit and exposed to Fuison solo.

## **2.9. Histological analysis**

Adult fish were fixed in Bouin's fixative overnight. After processing and paraffin embedding, 5  $\mu$ m sections were cut in either longitudinal or transverse sections. Staining was done with either hematoxylin and eosin

## **2.10. Embryo preparation and tumor cell implantation**

Dechorionized 2 days-post fertilization (dpf) tg(fli1:EGFP) zebrafish embryos were anaesthetized with 0.003% tricaine (containing phenylthiourea) and positioned on a 10-cm petri dish coated with 5% agarose. Single cell suspensions of fluorescent mammalian cells were re-suspended in PBS, kept at room temperature before implantation and implanted within 3h. Before injection, CM-Dil labeled cells were assessed for viability using trypan blue exclusion and only samples in which there

was >90% was viability used. The cell suspension was loaded into borosilicate glass capillary needles and the injections were performed using a pneumatic picopump and a manipulator (WPI, Stevenage, UK). Approximately 400 cells were injected at the ventral end of the duct of cuvier (DoC), where the DoC opens into the heart. After implantation with mammalian cells, zebrafish embryos were maintained at 33 °C .

### **2.11. Statistical analysis**

The data are expressed as the mean± standard error (SE), and one-way ANOVA test (using SPSS ver. 12 statistical software; SPSS Inc., Chicago, IL,USA) was used to compare the mean values of each treatment. Values with different alphabets are significantly different at  $p < 0.05$  as analyzed by Duncan's multiple range test.

### 3. RESULTS

#### 3.1. The establishment of liver and prostate tumor xenograft model in zebrafish

We observed to angiogenic activators, such as VEGFR2, TGF $\beta$ , MMP2, MMP9, TNF- $\alpha$ , and IL-6, cell metastasis and invasion, as well as histological staining for confirmed cancer levels. The angiogenic activators, including VEGFR2, TGF $\beta$ , MMP2, MMP9, TNF- $\alpha$ , and IL-6, were significantly increased in the zebrafish injected of Hep3B or Du145 cells ( $2 \times 10^6$ ,  $5 \times 10^6$  cells) in to their abdominal cavity once every three days for one month according to real-time PCR (Fig.3-1 and Fig.3-2). As shown Fig.3-3 and Fig.3-4 Hep3B and Du145 cells showed metastasis and invasion after xenografting by fluorescent microscopy. After 30 dpi, we observed tumor cells in liver, intestine, and abdominal muscles. Also, both cancer cell lines indicated a higher number of cells with increased levels of MMP2, TGF $\beta$ , p-VEGFR2 protein according to western blot analysis (Fig. 3-5A, Fig. 3-6A). Qualitative histological examinations of hepatic parenchyma vells stained with hematoxylin and eosin (H&E) revealed that the cell appeared to be less homogeneous in tumor than in the normal group (Ung et al., 2010). The  $5 \times 10^6$  cells groups (both cancer cell lines) indicated that liver parenchyma from cancer cell-treated groups appeared to be lost its intercellular contact and the cells were

dissociated within the tissue and were having irregular shape while normal liver cells were observed with well-delineated polygonal shape (Fig. 3-5B, Fig. 3-6B). AFP (alpha-fetoprotein) is used as a tumor marker to detect of hepatocellular carcinoma, germ cell tumors, and metastatic cancers of the liver. We found that AFP production in tumor cell-injected groups were increased  $2 \times 10^6$ ,  $5 \times 10^6$  cells, respectively (Fig. 3-5C). And prostate specific antigen (PSA) is often elevated in the presence of prostate cancer or other prostate disorders. Tumor cell-injected groups exhibited a dose-dependent induction in PSA levels. According to these results, the number of Hep3B and Du145 cells used in subsequent experiments were optimized as the  $5 \times 10^6$  cell-injected groups (Fig. 3-6C).

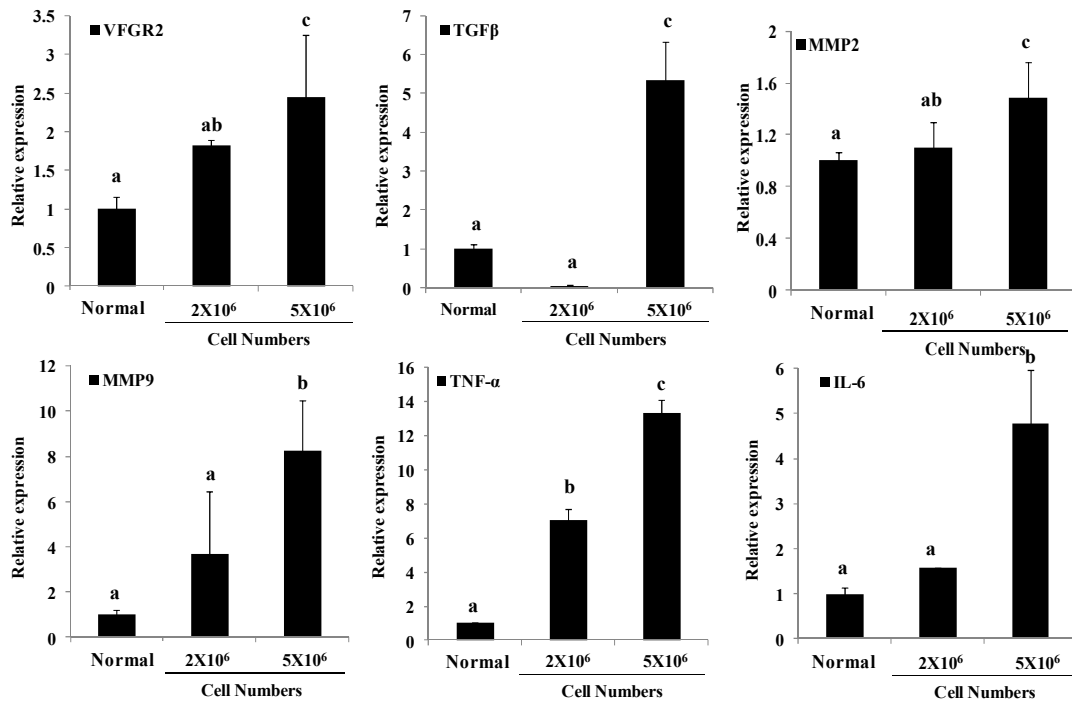


**Fig. 3-1.** The mRNA expression levels of VEGFR2, TGFβ, MMP2, MMP9, TNF-α and IL-6 revealed by rt-PCR in liver tumor xenograft zebrafish liver. The zebrafish were injected with 20 μl of Hep3B cells (2x10<sup>6</sup>, 5x10<sup>6</sup> cells) in to their abdominal cavity once every three days for one month. <sup>a-c</sup>Values with different alphabets are significantly different at p<0.05 as analyzed by Ducan’s multiple range test.

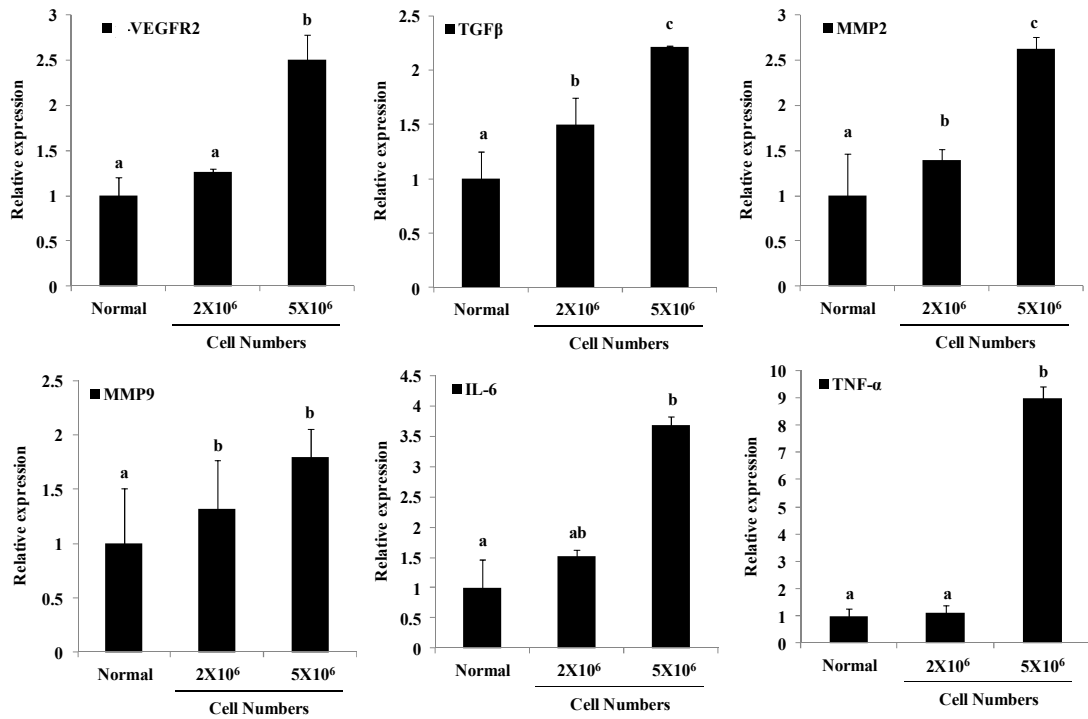


**Fig. 3-2.** The mRNA expression levels of VEGFR2, TGFβ, MMP2, MMP9, TNF-α and IL-6 revealed by rt-PCR in prostate tumor xenograft zebrafish liver. The zebrafish were injected with 20 μl of Du145 cells (2x10<sup>6</sup>, 5x10<sup>6</sup> cells) into their abdominal cavity once every three days for one month. <sup>a-c</sup>Values with different alphabets are significantly different at p<0.05 as analyzed by Duncan's multiple range test

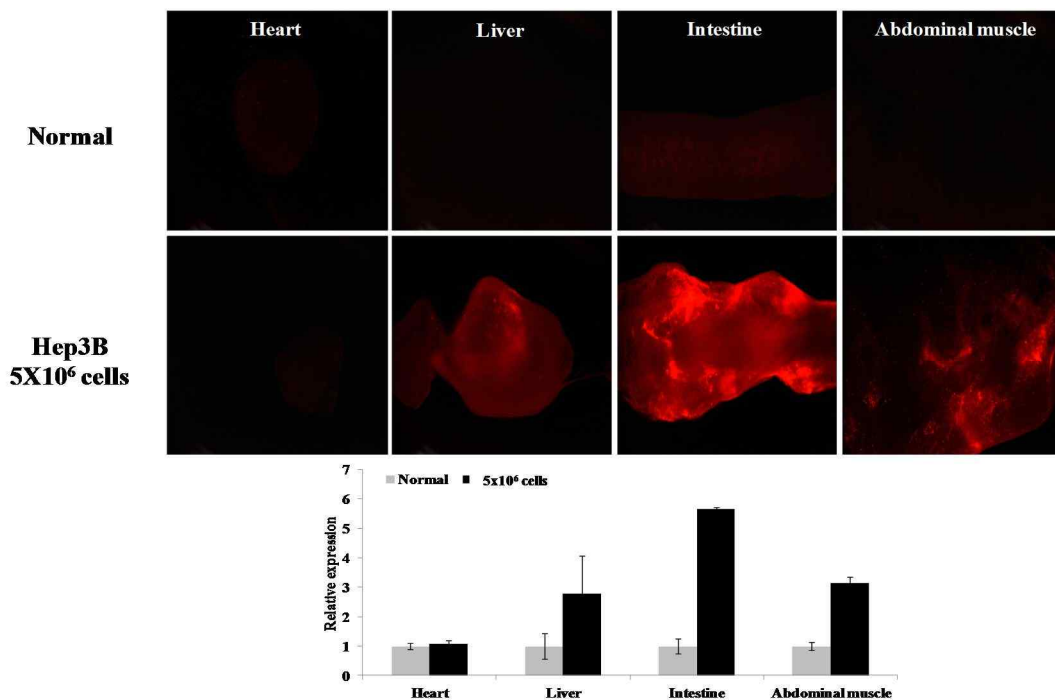


**Fig. 3-3. Liver tumor cells showing metastasis and invasion of a 30 dpi zebrafish after xenografted by fluorescent microscopic image.** Hep3B cells were stained with CM-Dil and injected into the abdominal cavity of zebrafish during ten times a month.

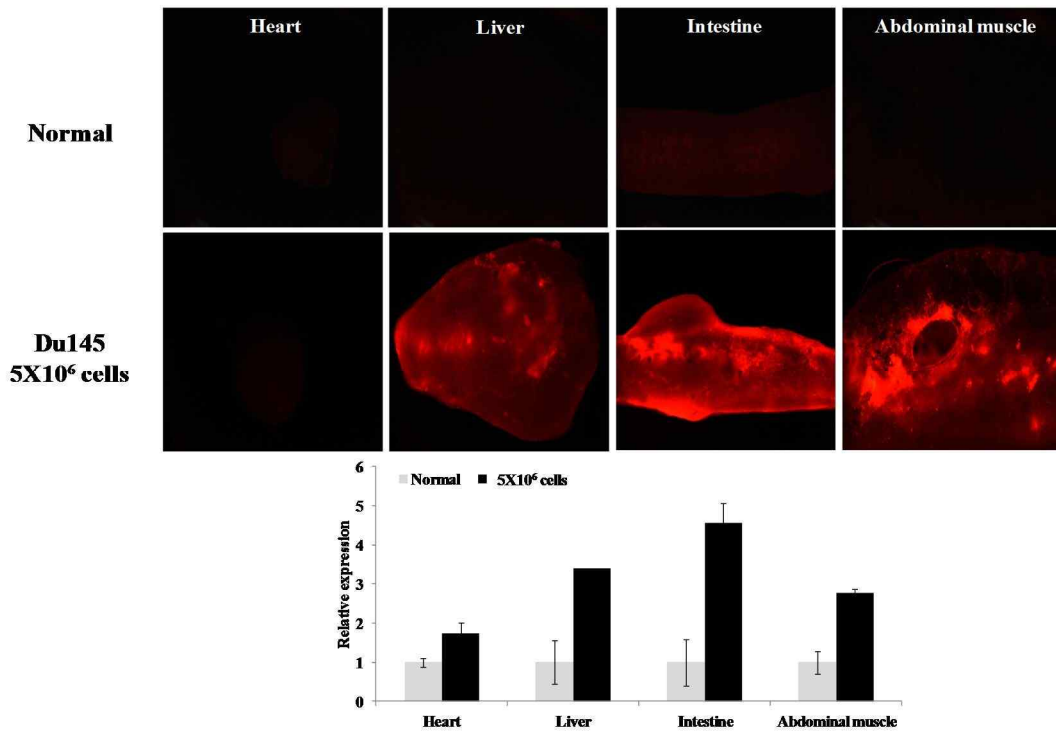


**Fig. 3-4. Prostate tumor cells showing metastasis and invasion of a 30 dpi zebrafish after xenografted by fluorescent microscopic image. Du145 cells were stained with CM-Dil and injected into the abdominal cavity of zebrafish during ten times a month.**

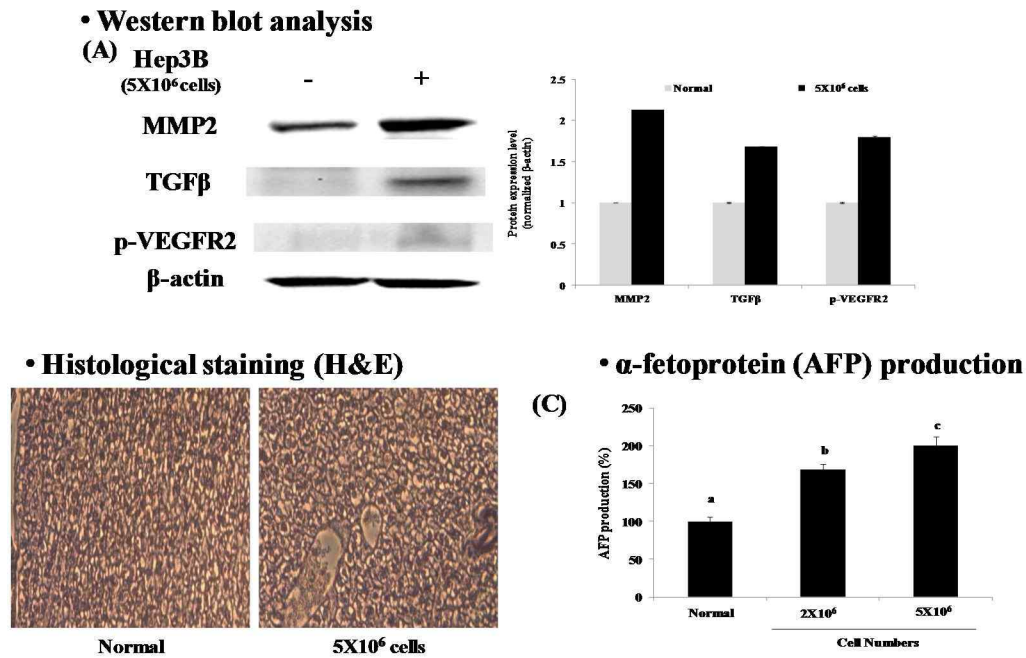


**Fig. 3-5. Measurement of cancer levels on protein expressions (MMP2, TGFβ, p-VEGFR2)(A), Histological staining (B) and α-fetoprotein production (C) by liver tumor xenograft zebrafish model** The zebrafish were injected with 20 μl of Hep3B (5x10<sup>6</sup> cells) in to their abdominal cavity once every three days for one month. <sup>a-</sup> Values with different alphabets are significantly different at p<0.05 as analyzed by Ducan's multiple range test.

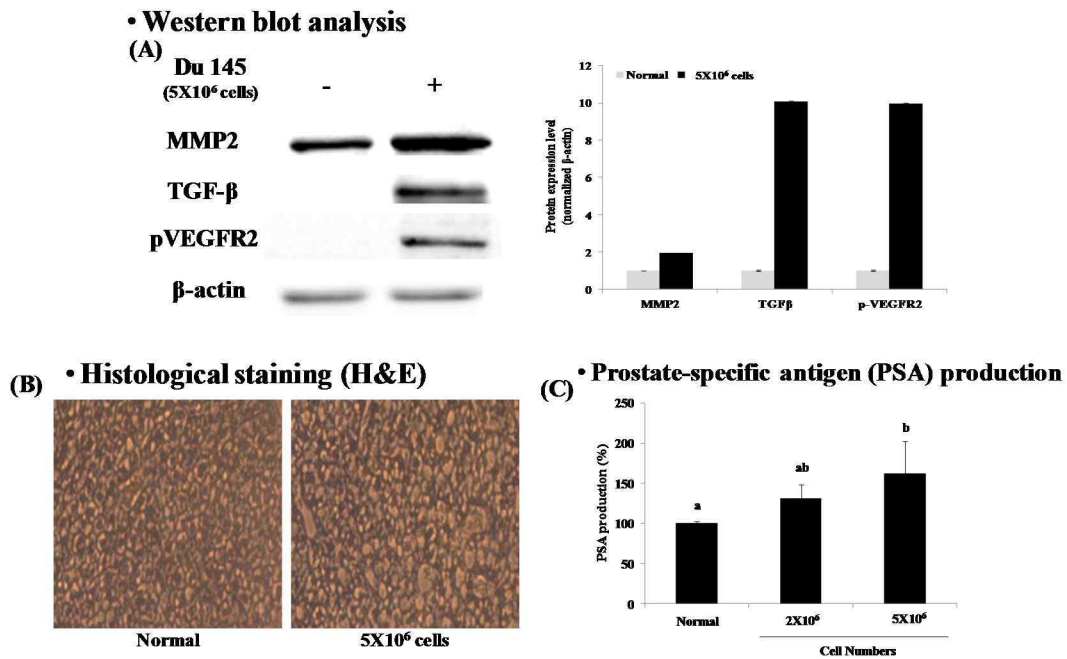


**Fig. 3-6. Measurement of cancer levels on protein expressions (MMP2, TGFβ, p-VEGFR2)(A), Histological staining (B) and prostate-specific antigen production (C) by prostate tumor xenograft zebrafish model. The zebrafish were injected with 20 μl of Du145 (5x10<sup>6</sup> cells) in to their abdominal cavity once every three days for one month. <sup>a-c</sup>Values with different alphabets are significantly different at p<0.05 as analyzed by Ducan's multiple range test.**

### **3-6. The potential anti-metastatic and anti-invasive effect of the SSA of *H.fusiforme* in liver and prostate tumor xenograft zebrafish model**

We established that anti-metastatic and anti-invasive properties could be achieved in cancer xenograft zebrafish models. Starting from the day zero the zebrafish were injected with SSA (2  $\mu\text{g/g}$  or 5  $\mu\text{g/g}$ ) once every three days. Starting from the day 7, the zebrafish were injected with 20  $\mu\text{l}$  of Hep3B or Du145 cells ( $5 \times 10^6$  cells) in to their abdominal cavity once every three days for one month continued with sample treatment. The survival rates 85% and 92% in the Hep3B cell-injected and Du145 cell-injected groups compared with the normal group. However, the survival rates of liver tumor xenograft zebrafish groups injected with SSA at 2  $\mu\text{g/g}$  and 5  $\mu\text{g/g}$  indicated a significant increase. SSA-injected group at 5  $\mu\text{g/g}$  indicated an increased survival rate in the prostate tumor xenograft zebrafish (Fig. 3-7A and Fig. 3-8A). And we confirmed to liver and prostates tumor marker. The AFP production of the Hep3B-injected group increased to 172% compared with that of the normal group. However, treatments with SSA significantly reduced AFP production (Fig. 3-7B). Also, The PSA production of the Du145-injected group increased to 148% compared with that of the normal group. Besides, SSA treatments dose-dependently reduced the PSA production (Fig. 3-8B). As shown in Fig. 3-9 and Fig. 3-10, Hep3B and Du145

cells showed metastasis and invasion after xenografting by fluorescent microscopy. After 30 dpi, we observed tumor cells in liver and intestine, abdominal muscles expect heart. However the SSA treatment effectively inhibited the metastasis and invasion in liver and intestine, abdominal muscles. Qualitative histological examinations with hematoxylin and eosin (H&E) revealed the  $5 \times 10^6$  cancer cells-injected groups (Hep3B cells or Du145 cells) observed to be lost its intercellular contact and the cells were dissociated within the tissue and were having irregular shape while normal liver cells were observed with well-delineated polygonal shape. However, SSA-injected groups at 2  $\mu\text{g/g}$  and 5  $\mu\text{g/g}$  had remarkably reduced the intercellular contact and the cells were dissociated within the tissue with irregular shape (Fig. 3-11 and Fig. 3-12). The angiogenic activators, including VEGFR2, TGF $\beta$ , MMP2, MMP9, TNF- $\alpha$ , and IL-6, were remarkably increased in the zebrafish injected with Hep3B or Du145 cells ( $5 \times 10^6$  cells) according to real-time PCR. But, the treatments with SSA at a 5  $\mu\text{g/g}$  significantly reduced all angiogenic activators (Fig. 3-13 and Fig. 3-14). Hep3B or Du145 cells-injected groups considerably increased MMP2 expression. But SSA-injected group indicated a reduced MMP2 expression with concentration-dependent manner (Fig. 3-15. and Fig. 3-16). We confirmed the effect of SSA on PI3K/Akt/mTOR pathway in liver and prostate tumor

xenograft zebrafish model. As shown in Fig. 3-15. and Fig. 3-16, The Hep3B and Du145 cells-injected groups increased PI3K, Akt, and mTOR phosphorylation. Moreover, phosphorylation of PI3K, Akt and mTOR was effectively inhibited by SSA-injected group, respectively.

We confirmed that Hep3B and Du145 cancer cells with CM-Dil labels could disseminate the zebrafish embryos model *in vivo* and SSA suppressed invasion/metastasis of cancer cells. CM-Dil labeled Hep3B or Du145 cells were injected into the Doc of 2 dpf embryos and analyzed at 4 dpf using fluorescence microscopy. Dual fluorescent images displayed irregular green neovessels in red tumor cells in cancer cell injected group. But SSA 12.5  $\mu\text{g/ml}$  treated group showed a regular green vessels and a reduced amount of cancer cells (Fig. 3-17 and Fig. 3-18).

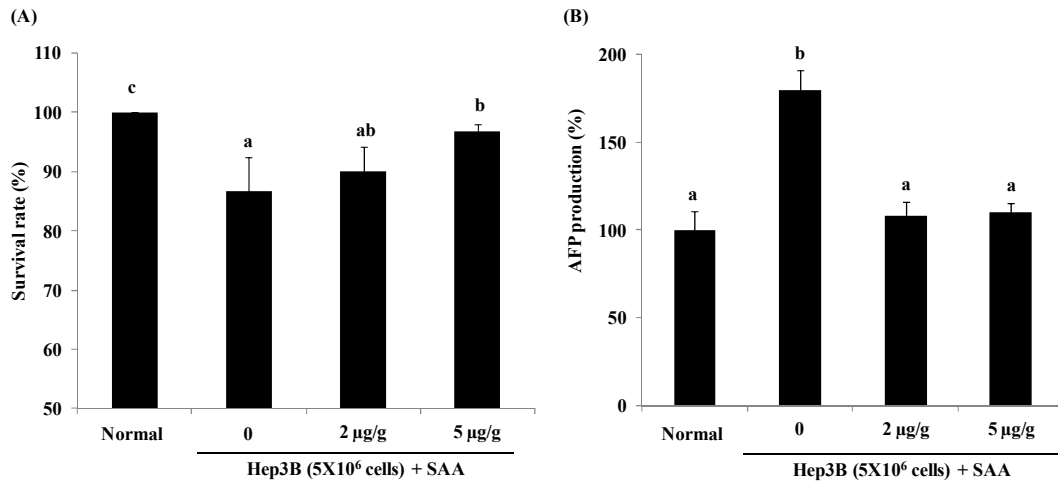


**Fig. 3-7. The effect of the intramuscular injection of SSA on survival rate (A) and a-fetoprotein production (B) in liver tumor xenograft zebrafish model.** Starting from the day zero the zebrafish were injected with SSA (2 μg/g or 5 μg/g) once every three days. Starting from the day 7, the zebrafish were injected with 20 μl of Hep3B cells (5x10<sup>6</sup> cells) in to their abdominal cavity once every three days for one month. <sup>a-c</sup>Values with different alphabets are significantly different at p<0.05 as analyzed by Ducan's multiple range test.

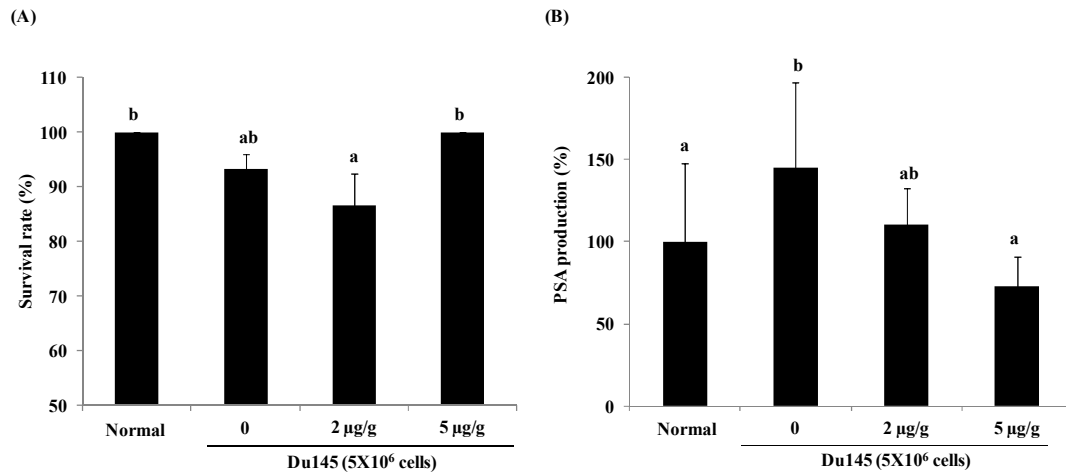


**Fig. 3-8. The effect of the intramuscular injection of SSA on Survival rate (A) and prostate-specific antigen production (B) in prostate tumor xenograft zebrafish model.** . Starting from the day zero the zebrafish were injected with SSA (2 μg/g or 5 μg/g) once every three days. Starting from the day 7, the zebrafish were injected with 20 μl of Du145 cells (5x10<sup>6</sup> cells) in to their abdominal cavity once every three days for one month continued with sample treatment. <sup>a-c</sup>Values with different alphabets are significantly different at p<0.05 as analyzed by Ducan’s multiple range test.

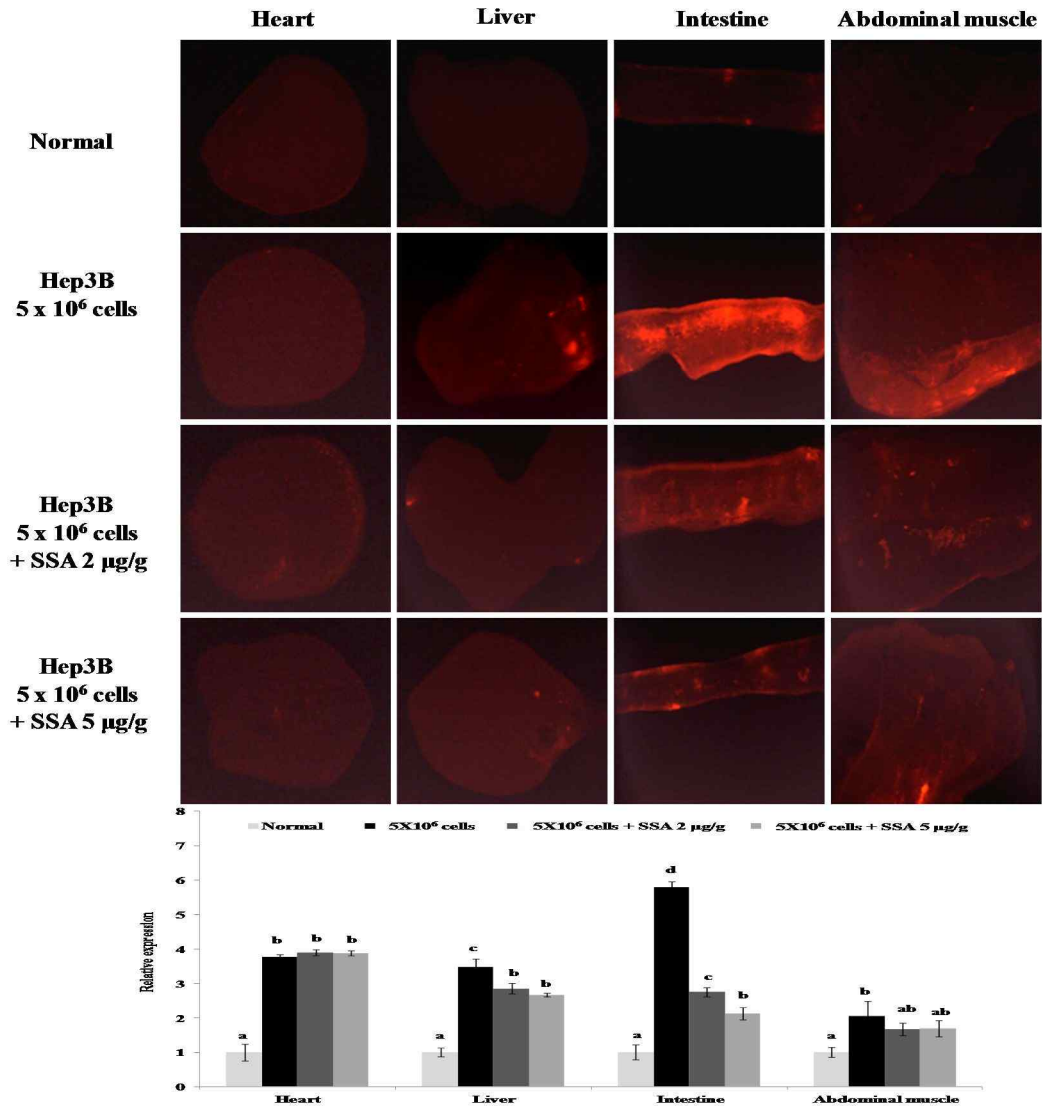


**Fig. 3-9. The effect of SSA on metastasis and invasion in liver tumor xenograft zebrafish model by fluorescent microscopic images.** Starting from the day zero the zebrafish were injected with SSA (2 µg/g or 5 µg/g) once every three days. Starting from the day 7, the zebrafish were injected with 20 µl of Hep3B cells (5x10<sup>6</sup> cells) in to their abdominal cavity once every three days for one month continued with sample treatment multiple range test.

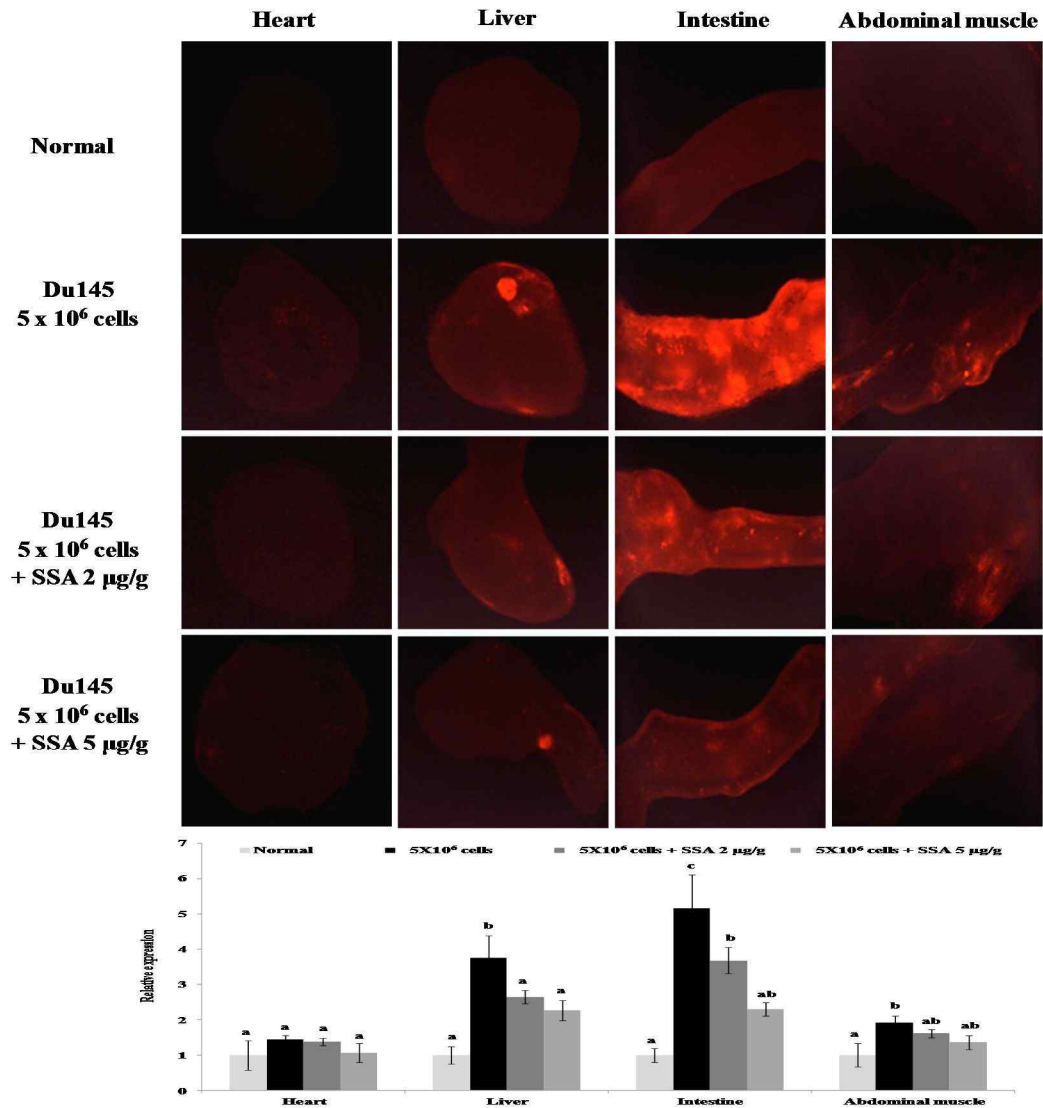


**Fig. 3-10. The effect of SSA on metastasis and invasion in prostate tumor xenograft zebrafish model by fluorescent microscopic images.** Starting from the day zero the zebrafish were injected with SSA (2 µg/g or 5 µg/g) once every three days. Starting from the day 7, the zebrafish were injected with 20 µl of Du145 cells (5x10<sup>6</sup> cells) in to their abdominal cavity once every three days for one month continued with sample treatment multiple range test.

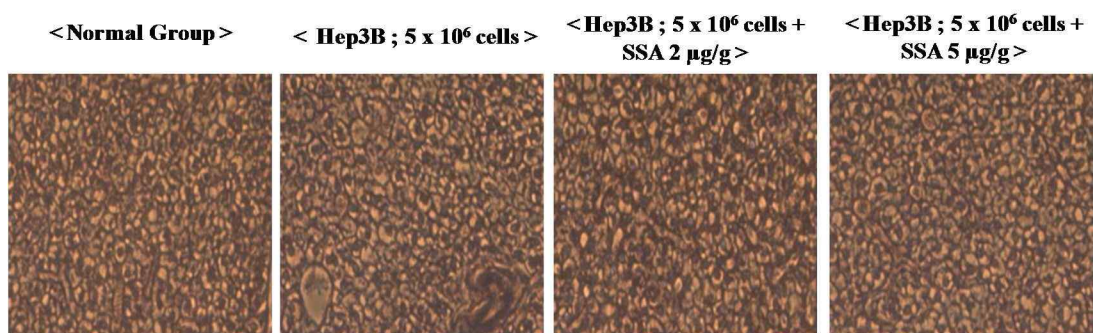


**Fig. 3-11. The effect of SSA on H&E (Hematoxylin & Eosin) staining in liver tumor xenograft zebrafish model.** Starting from the day zero the zebrafish were injected with SSA (2 μg/g or 5 μg/g) once every three days. Starting from the day 7, the zebrafish were injected with 20 μl of Hep3B cells (5x10<sup>6</sup> cells) in to their abdominal cavity once every three days for one month continued with sample treatment.

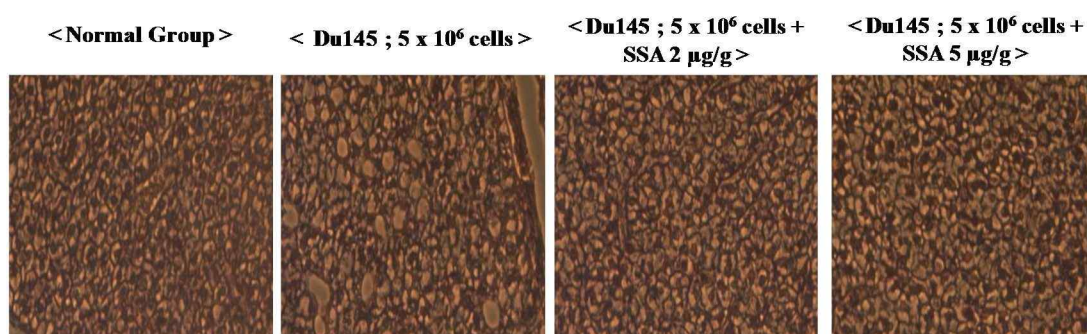


**Fig. 3-12. The effect of SSA on H&E (Hematoxylin & Eosin) staining in prostate tumor xenograft zebrafish model.** Starting from the day zero the zebrafish were injected with SSA (2 μg/g or 5 μg/g) once every three days. Starting from the day 7, the zebrafish were injected with 20 μl of Du145 cells (5x10<sup>6</sup> cells) in to their abdominal cavity once every three days for one month continued with sample treatment.

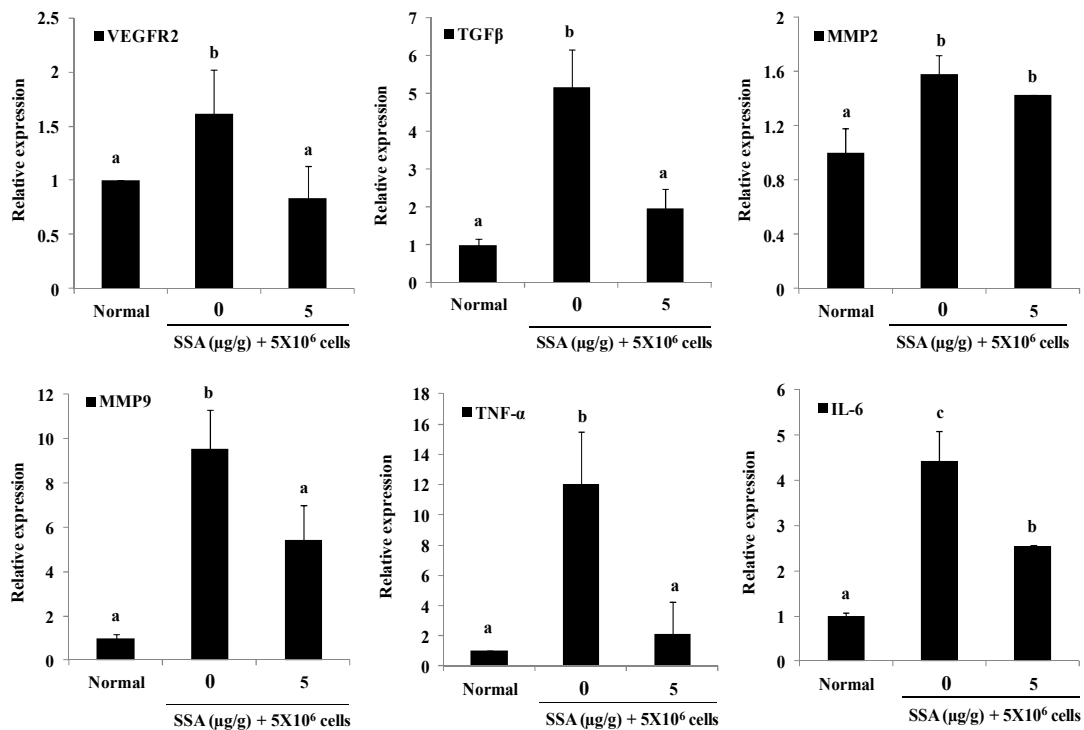


**Fig. 3-13.** The mRNA expression levels of VEGFR2, TGFβ, MMP2, MMP9, TNF-α and IL-6 revealed by rt-PCR in liver tumor xenograft zebrafish liver.

Starting from the day zero the zebrafish were injected with SSA (2 μg/g or 5 μg/g) once every three days. Starting from the day 7, the zebrafish were injected with 20 μl of Hep3B cells (5x10<sup>6</sup> cells) in to their abdominal cavity once every three days for one month continued with sample treatment. <sup>a-c</sup>Values with different alphabets are significantly different at p<0.05 as analyzed by Ducan’s multiple range test .

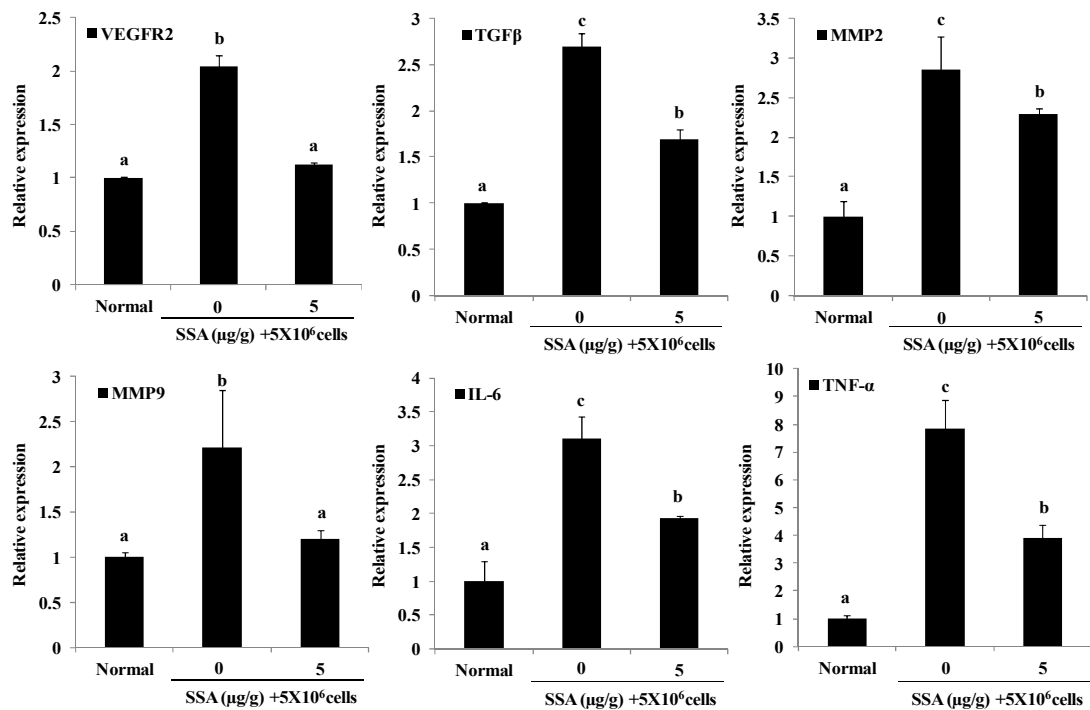


**Fig. 3-14. The mRNA expression levels of VEGFR2, TGFβ, MMP2, MMP9, TNF-α and IL-6 revealed by rt-PCR in prostate tumor xenograft zebrafish liver.**

Starting from the day zero the zebrafish were injected with SSA (2 μg/g or 5 μg/g) once every three days. Starting from the day 7, the zebrafish were injected with 20 μl of Du145 cells (5x10<sup>6</sup> cells) in to their abdominal cavity once every three days for one month continued with sample treatment. <sup>a-c</sup>Values with different alphabets are significantly different at p<0.05 as analyzed by Ducan's multiple range test .

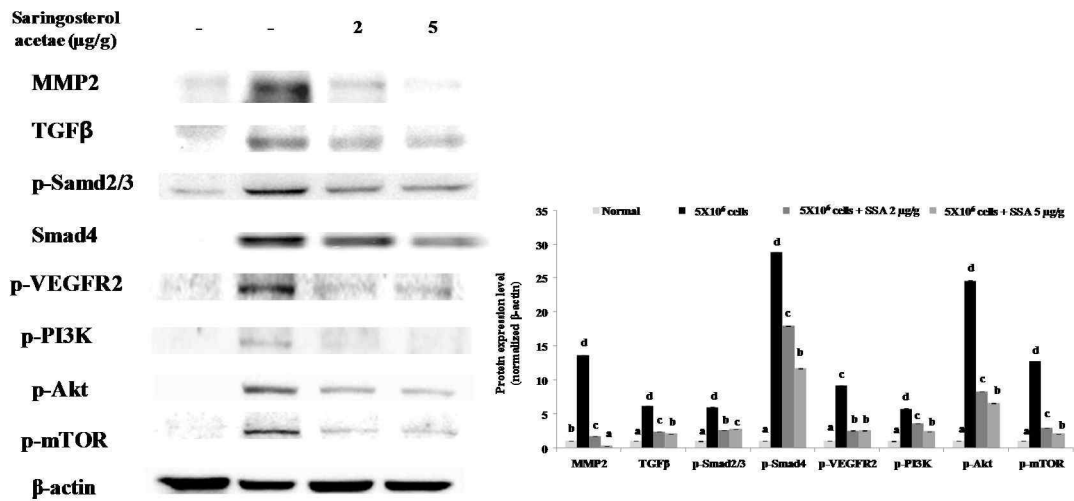


**Fig. 3-15.** The protein expression levels of MMP2, TGFβ pathway and PI3K/Akt/mTOR pathway revealed by western blot analysis in liver tumor xenograft zebrafish liver. Starting from the day zero the zebrafish were injected with SSA (2 μg/g or 5 μg/g) once every three days. Starting from the day 7, the zebrafish were injected with 20 μl of Hep3B (5x10<sup>6</sup> cells) in to their abdominal cavity once every three days for one month continued with sample treatment. <sup>a-</sup> Values with different alphabets are significantly different at p<0.05 as analyzed by Ducan's multiple range test

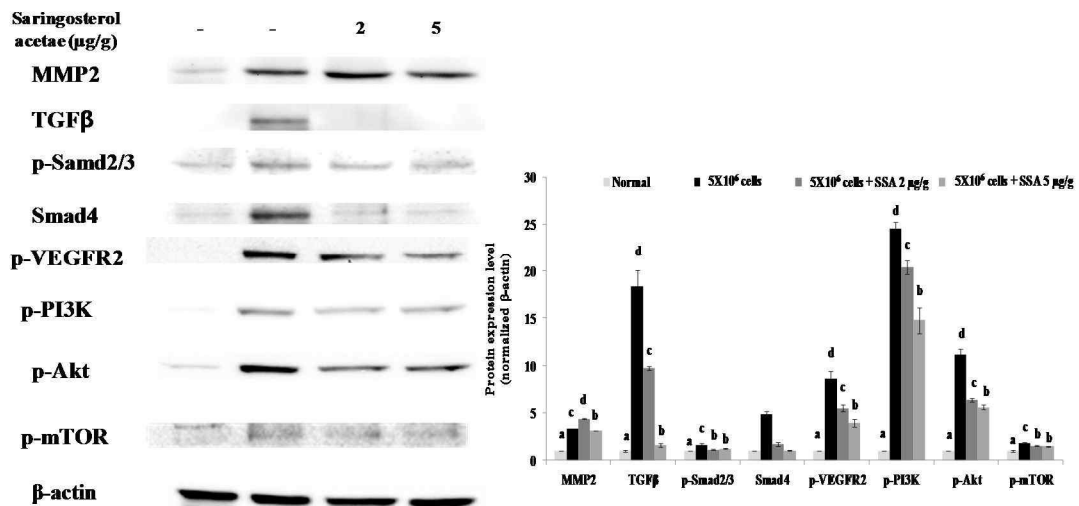


**Fig. 3-16.** The protein expression levels of MMP2, TGFβ pathway and PI3K/Akt/mTOR pathway revealed by western blot analysis in prostate tumor xenograft zebrafish liver. Starting from the day zero the zebrafish were injected with SSA (2 μg/g or 5 μg/g) once every three days. Starting from the day 7, the zebrafish were injected with 20 μl of Du145 cells (5x10<sup>6</sup> cells) in to their abdominal cavity once every three days for one month continued with sample treatment. <sup>a-</sup> Values with different alphabets are significantly different at p<0.05 as analyzed by Ducan's multiple range test.

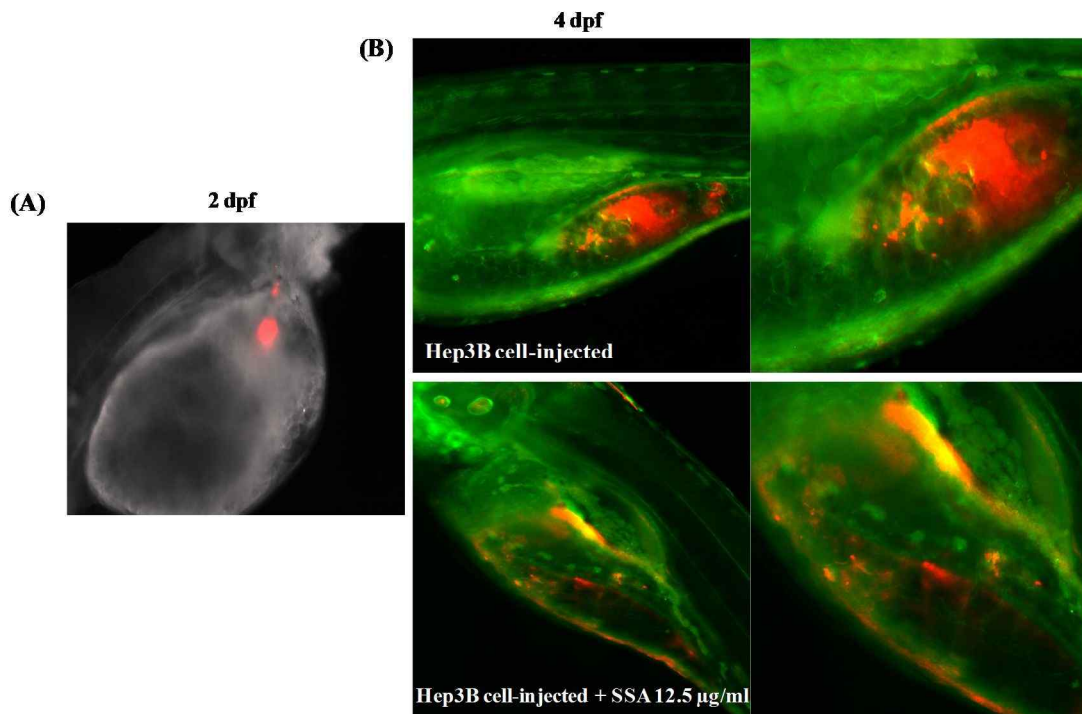


**Fig. 3-17. Tumor xenografts in zebrafish embryo. Labeled hepatocellular carcinoma Hep3B cells were injected to transgenic *tg(fli1:EGFP)* zebrafish embryo at 48 hpf. Then the embryos were analyzed by fluorescence microscopy. Brightfield image of Hep3B cells inside the *tg(fli1:EGFP)* transgenic zebrafish embryo at 0 dpi (A). Fluorescence imaging of the embryo at 48 hpi showing interaction between the vasculature (labeled green) and the tumor cells (labeled red) (B).**

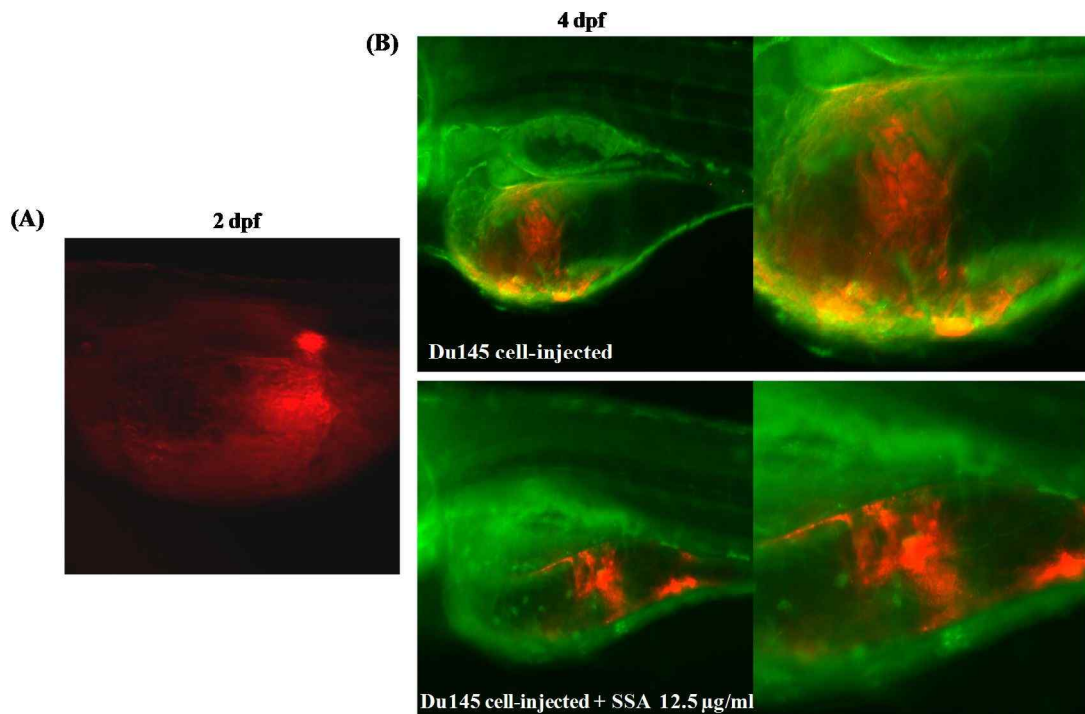


**Fig. 3-18. Tumor xenografts in zebrafish embryo. Labeled prostate carcinoma Du145 cells were injected to transgenic *tg(fli1:EGFP)* zebrafish embryo at 48 hpf. Then embryos were analyzed by fluorescence microscopy. Brightfield image of Du145 cells inside the *tg(fli1:EGFP)* transgenic zebrafish embryo at 0 dpi (A). Fluorescence imaging of the embryo at 48 hpi showing interaction between the vasculature (labeled green) and the tumor cells (labeled red)(B).**

#### 4. DISSUSIONS

Angiogenesis is required for invasive tumor growth and metastasis and considered to be an important point in the control of cancer progression (Folkman 2002).

Metastasis, rather than primary tumors, are responsible for most cancer deaths, cancer cells metastasis is a complex multistep process involving cell adhesion, motility (migration) and invasion. Hence, interruption of one or more of these steps is one approach for anti-metastatic therapy (Nam and Shon, 2009).

Tumor growth and metastasis depends on angiogenesis and lymphangiogenesis triggered by chemical signals from tumor cells in a phase of rapid growth (Folkman 1971). More than a dozen different proteins have been identified as angiogenic activators, including vascular endothelial growth factor (VEGF), angiogenin, transforming growth factor (TGF $\beta$ ), interleukin-6 (IL-6), tumor necrosis factor (TNF- $\alpha$ ), metalloproteinases (MMPs). The VEGF family and their receptors (VEGFR) are receiving increasingly more attention in the field of neoplastic vascularization. Among the VEGF forms, VEGF-A is an important driver of neovascular growth required to support solid tumor progression. The primary signaling receptor for VEGF-A is VEGF receptor (VEGFR)-2, and activation of VEGFR-2 by VEGF-A on endothelial tip and stalk cells directs the migration and

extension of sprouting vessels, respectively (Smith et al., 2003). The MMPs destroy the extracellular matrix which fills the spaces between cells and is made of protein and polysaccharides. This matrix permits the migration of endothelial cells. The endothelial cell begins to separate as they migrate into the surrounding tissues (Nishida et al., 2006). TNF- $\alpha$ , a core cytokine produced by immune cells in the blood stream, acts, as pro-angiogenic factor (Naldini and Carraro., 2005). IL-6 is involved in the host immune defense mechanism as well as the modulation of growth and differentiation in various malignancies (Guo et al., 2012). Therefore, in this study, we confirmed the angiogenic activators according to the important role they play in angiogenesis. These activator that include VEGFR2, TGF $\beta$ , MMP2, MMP9, TNF- $\alpha$ , and IL-6, were increased according to a dose-dependent induction in the zebrafish injected with Hep3B or Du145 cells ( $2 \times 10^6$ ,  $5 \times 10^6$  cells) in to their abdominal cavity once every three days for one month (Fig. 3-1 and Fig. 3-2). Also, Hep3B or Du145 cells ( $2 \times 10^6$ ,  $5 \times 10^6$  cells) indicated metastatic and invasion effects after the cells were stained with CM-Dil and injected into the abdominal cavity of zebrafish during ten times a month to liver, intestine, and abdominal muscles (Fig. 3-9 and Fig. 3-10). Liver cancer marker (AFP) and prostate cancer marker (PSA) exhibited a dose-dependent induction (Fig. 3-5B, Fig. 3-6B) in zebrafish. Therefore, a tumor cell-

injected group of  $5 \times 10^6$  cells (Hep3B or Du145 cells) can be considered as a lethal concentration that finally results in cancer.

We examined the potential anti-metastatic and anti-invasive effects of SSA in xenograft zebrafish model. Both angiogenic activators and tumor markers (AFP and PSA) were reduced by injection of SSA (2  $\mu\text{g/g}$  and 5  $\mu\text{g/g}$ ) to Hep3B or Du145 cell ( $5 \times 10^6$  cells)-injected zebrafish (Fig. 3-7, Fig. 3-8, Fig. 3-13 and Fig. 3-14). Also, SSA inhibited the invasion and the metastasis of cancer cells in CM-Dil labeled adult zebrafish in liver, intestine, and abdominal muscles and tg(fli1:EGFP) transgenic zebrafish embryos (Fig. 3-9, Fig. 3-10, Fig. 3-17 and Fig. 3-18).

MMPs plays an essential role in many aspects of biology, such as cell proliferation, differentiation, apoptosis and migration, and the speed up of MMPs have clear links to tumor growth, invasion, and metastasis. Among MMPs, MMP2 is closely correlated with tumor progression, angiogenesis and metastasis (Liu et al., 2015, Verma et al., 2014, Nelson et al., 2000). The endothelial cells begin to divide as they migrate into the surrounding tissues. TG- $\beta$  maintains tissue homeostasis and prevents incipient tumors from progressing down the path to malignancy by regulating not only cellular proliferation, differentiation, survival, and adhesion but also the cellular microenvironment. (Massague., 2008). The abnormal activation of the

phosphatidylinositol 3-kinase (PI3K)/Akt (Akt also known as protein kinase (PKB)) pathway has been validated by epidemiological and experimental studies as an essential step towards the initiation and maintenance of human tumors. We confirmed the effect of SSA on MMP2, TGF $\beta$  pathways and PI3K/Akt/mTOR pathways in liver and prostate tumor xenograft zebrafish model of liver. Since SSA was able to effectively inhibit the MMP2, phosphorylation TGF $\beta$  pathway and phosphorylation PI3K/Akt/mTOR pathway compared to Hep3B or Du145 injected group, respectively (Fig. 3-15 and Fig. 3-16). Therefore, SSA could be the reason of preventing tumor progression, angiogenesis and metastasis.

## 5. CONCLUSION

In conclusion, this zebrafish model can be used as an *in vivo* experiment to confirm the anti-metastatic and anti-invasive effects. And saringosterol acetate isolated from *H. fusiforme* could be the reason of preventing tumor progression, angiogenesis and metastasis. Therefore, SSA has the potential to be used as an ingredient in nutraceuticals or functional food to reduce carcinogenic effects

## REFERENCES

- Barrow C., Shahidi F., Marine nutraceuticals and functional foods. 2008, New York, CRC Press.
- Chico Timothy J.A., Ingham Philip W., Crossman David C., Modeling cardiovascular disease in the zebrafish. *Trends in Cardiovascular Medicine*, 2008, 18, 150-155.
- Detrich H. The zebrafish: disease models and chemical screens. *Methods in cell biology*. 2011, 105.
- Eisen Judith S. Zebrafish make a big splash. *Cell*, 1996, 87, 969-977.
- Feitsma Harma and Cuppen Edwin. Zebrafish as a cancer model. *Molecular Cancer Research*, 2008, 6, 685-694.
- Folkman Judah. Tumor angiogenesis: therapeutic implications. *The New England Journal of Medicine*, 1971, 285, 1182-1186.
- Folkman Judah, Role of angiogenesis in tumor growth and metastasis. *Seminars in Oncology*. 2002, 29, 15-18.
- Gleeson M., Connaughto C., Arneson I. S., Induction of hyperglucemia in zebrafish (*Danio rerio*) leads to morphological changes in the retina. *Acta Diabetologica*, 2007, 44, 157-163.
- Guo Yuqi, Zu Feng, Lu TianJian, Duan Zhenfeng, Zhang Zhan. Interleukin-6

signaling pathway in targeted therapy for cancer. *Cancer Treatment Reviews*. 2012, 38, 904-910.

Halliwell B., Gutteridge J.M.C. Antioxidant defenses. In: *Free radicals in biology and medicine*. Oxford Science Publication, Oxford, UK, 1999, 3<sup>rd</sup> ed. Pp. 105-159.

Han Yu Ran, Ali Md. Yousof, Woo Mi-Hee, Jung Hyun Ah, Choi Jae Sue. Anti-diabetic and anti-inflammatory potential of the edible brown alga *Hizikia fusiformis*. *Journal of Food Biochemistry*. 2015, 39, 417-428.

Heo Soo-Jin, Park Eun-Ju, Lee Ki-Wan, Jeon You-Jin, Antioxidant activities of enzymatic extracts from brown seaweed. *Bioresource Technology*, 2005a, 96, 1613-1623.

Heo Soo-Jin, Park Pyo-Jam, Park Eun-Ju, Kim Se-kwon, Jeon You-Jin. Antioxidant activity of enzymatic extracts from a brown seaweed *Ecklonia cava* by electron spin resonance spectrometry and comet assay. *European Food Research and Technology*, 2005b, 221, 41-47.

Howe Kerstin, Clark Matthew D., Torroja Carllose F., Torrance James, Berthelot Camile, Muffato Matthieu, Collins John E., Humphray Sean, McLaren Karen, Matthews Lucy et al. The zebrafish reference genome sequence and its relationship to the human genome. *Nature*, 2013, 496, 498-503.

Hsu Chi-Hsin, Wen Zhi-Hong, Lin Chan-Shing, Chakraborty Chiranjib. The zebrafish model: use in studying cellular mechanisms for a spectrum of clinical disease entities. *Current Neurovascular Research*, 2007, 4, 111-120.

Jemal Ahmedin, Center Melissa M., Desantis Carol, Ward Elizabeth M., Global Patterns of cancer incidence and mortality rates and trends. *American Association for Cancer Research*, 2010, 19, 1893-1907.

Jing Lili, Zon Leonard I. Zebrafish as a model for normal and malignant hematopoiesis. *Disease model & Mechanisms*, 2011, 4, 433-438.

Kent ML, Spitsbergen JM, Matthews JM, Fournie JW, Westerfield M. Diseases of zebrafish in research facilities. *Zebrafish International Resource Center*. 2002, available from: <http://zebrafish.org/zirc/health/diseaseManual.php>.

Kim Kyung-Im, Seo Hae-Duk, Lee Hyun-Sun, Jo Hong-Yeon, Yang Han-Chul. Studies on the blood anticoagulant polysaccharide isolated from hot water extracts of *Hizikia fusiform*. *Journal of the Korean Society of Food Science and Nutrition*. 1998, 27, 1204-1210.

Komura Takeshi, Wada Setsu, Nagayama hideo. The identification of fucosterol in the marine brown algae *Hizikia fusiformis*. *Agricultural and Biological Chemistry*. 1974, 38, 2275-2276.

Lan Chuan-Ching, Tang Rongying, Leong Ivone Un San, Love Donald R. Quantitative real-time rt-pcr (qrt-pcr) of zebrafish transcripts: optimization of rna extraction, quality control considerations, and data analysis. Cold Spring Harb Protocols. 2009, 10, 5314.

Lee Ji-Hyeok, Ko Ju-Young, Samarakoon Kalpa, Oh Jae-Young, Heo Soo-Jin, Kim Chul-Young, Nah Jae-Woon, Jang Mi-Kyeong, Lee Jung-Suck, Jeon You-Jin. Preparative isolation of sargachromanol E from *Sargassum siliquasterum* by centrifugal partition chromatography and its anti-inflammatory activity. Food and Chemical Toxicology, 2013, 62, 54-60.

Li Tongyuan, Kon Ning, Jiang Le, Tan Minjia, Ludwig Thomas, Zhao Yingming, Baer Richard, Gu Wei. Tumor suppression in the absence of p53 mediated cell cycle arrest, apoptosis, and senescence. Cell. 2012, 149, 1269-1283.

Liu qinghua, Pan Donghui, Cheng Chao, Zhang Anyu, Ma Chao, Wang Lizhen, Shang Dazhi, Liu Hongrui, Jiang Hongdie, Wang Tao, Xu Yuping, Yang Runlin, Chen Fei. Targeting of MMP2 activity in malignant tumors with a <sup>68</sup>Ga-labeled gelatinase inhibitor cyclic peptide. Nuclear Medicine and Biology, 2015, 42, 939-944.

Lockhart A. Craig, Braun Rod D., Yu Daohai, Ross Joel R. Dewhirst Mark W., Humphrey Jeffrey S., Thompson Seth, Williams Kathleen M., Klitzman Bruce, Yuan

Fan, Grichnik James M., Proia Alan D., Conway Delina A, Hurwitz Herbert I.,  
Reduction of wound Angiogenesis in patients Treated with BMS-275291, a broad  
spectrum matrixmetalloproteinase inhibitor. *Clinical Cancer Research*, 2003, 9, 586-  
593.

Massague Joan. TGF $\beta$  in cancer. *Cell*. 2008, 134, 215-230.

Morgan Claire, Lewis paul D, Hopkins Lynda, Burnell Stephamie, Kynaston  
Howard, Doak Shareed H. Increased expression of ARF GTPases in prostate cancer  
tissue. *Springer Plus*. 2015, 4, 342-345.

Naldini Antonella, Carraro Fabio. Role of inflammatory mediators in angiogenesis.  
*Current Drug Target inflammation & Allergy*. 2005, 4, 3-8.

Nam Kyung-Soo, Shon Yun-Hee. Suppression of metastasis of human breast cancer  
cells by chitosan oligosaccharides. *Journal of Microbiology and Biotechnology*. 2009,  
19, 629-633.

Nelson Amy R., Fingleton Barbara, Rothenberg Mace L. Matrisian Kynn M. Matrix  
Metalloproteinases: Biologic activity and clinical implications. *Journal of Clinical  
Oncology*.. 2000, 18, 1135-1149.

Nicoletti I., Migliorati G., Pagliacci M.C., Grignani F., Riccardi C., A rapid and  
simple method for measuring thymocyte apoptosis by propidium iodide staining and

flow cytometry. *Journal of Immunological Methods*, 1991, 139, 271-279.

Nishida Naoyo, Yano Hirohisa, Nishida Takashi, Kamura Toshiharu, Kojiro Masamichi. Angiogenesis in cancer. *Vascular Health and Risk Management*, 2006, 2, 213-219.

Permeah parisa, Saeidnia Soodabeh, Mashinchian-Moradi Ali, Gohari Ahmad R. Sterols from *Sargassum oligocystum*, a brown algae from the Persian gulf, and their bioactivity. *Natural Product Research*. 2012, 26, 774-777.

Siriwardhana Nalin, Lee Ki-wan, Kim Se-Kwon, Ha Jin-Won, Jeon You-Jin. Antioxidant activity of *Hizikia fusiformis* on reactive oxygen species scavenging and lipid peroxidation inhibition. *Food Science and Technology International*. 2003, 9, 339-346.

Smith Caroline L. Birdsey Graeme M. Anthony Shelagh, Anthony Shelagh, Arrigoni Francesca I., Leiper James M., Vallance Patrick. Dimethylarginine dimethylaminohydrolase activity modulates ADMA levels, VEGF expression, and cell phenotype. *Biochemical and Biophysical Research Communications*, 2003, 308, 984-989.

Spano Daniela, Heck Chantal, Antonellis Pasqualino De, Christofori Gerhard, Zollo Massimo. Molecular networks that regulate cancer metastasis. *Seminars in Cancer*

Biology. 2012, 22, 234-249.

Stewart Adam Michael, Braubach Oliver, Spitsbergen Jan, Gerlai Robert, Kalueff

Allan V. Zebrafish models for translational neuroscience research: from tank to bedside. Cellpress, 2014, 37, 1-15.

Teng Yong, Xie Xiayang, Walker Stenven, White David T, Mumm Jeff S, Cowell

John K. Evaluating human cancer cell metastasis in zebrafish. BMC Cancer, 2013, 13, 1-12.

Vara Juan Angel Fresno, Casado Enrique, Castro Javier de, Cejas Paloma, Belda-

Iniesta Cristobal, Gonzalez-Baron Manuel. PI3K/Akt signaling pathway and cancer. Cancer Treatment Reviews, 2004, 30 193-204.

Verma Sygreev, Kesh Kousik, Ganguly Nilanjan, Jana Sayantan, Swarmaker

Snehasikta. Matrix metalloproteinases and gastrointestinal cancer: impacts of dietary antioxidants. World Journal of Biological Chemistry, 2014, 5, 355-376.

Wajant Harald. The Role of TNF in Cancer. Death Receptors and Cognate Ligands in Cancer. 2009, 49, 1-15.

Zhu Tao, Heo Hyo Jung, Row Kyung Ho. Optimization of crude polysaccharides extraction from *Hizikia fusiformis* using response surface methodology. Carbohydrate Polymers. 2010, 82, 160-110.

## ACKNOWLEDGEMENT

학부 4학년말에 연구실에 들어와 석사, 박사과정을 큰 문제 없이 결실을 얻을 수 있게 도와주신 모든 분의 관심과 도움에 대한 표현을 이 자리를 빌어 감사의 말씀을 드리하고자 합니다. 항상 바른길로 갈 수 있게 사랑과 격려를 아끼시지 않은 우리 전유진교수님, 몸과 마음이 지쳐 있을 때 교수님의 응원과 칭찬으로 힘을 얻게 해주시고, 항상 밝은 미소로 맞이해 주시는 교수님이 계셔서 제가 자신이 없어 안될 것 같던 일도 교수님이 주시는 관심과 사랑으로 모든 일을 이겨 낼 수 있었습니다. 늘 존경하는 마음은 가득하지만 이번 기회를 빌려 표현합니다. 바른길로, 좋은 길로 인도해 주셔서 감사합니다. 그리고 대학원 기간 동안 전공적인 지식과 조언을 해주셔서 논문이 좀 더 나은 방향으로 나갈 수 있게 도와주신 이기완 교수님, 송춘복 교수님, 최광식 교수님, 이제희 교수님, 허문수 교수님, 여인규 교수님, 이경준 교수님, 정준범 교수님, 김기영 교수님, 이승헌 교수님께 감사 드립니다.

사랑하는 해양생물자원이용공학 연구실 가족, 연구실에서 함께 생활하지 않은 저에게도 관심과 격려로 많은 힘을 주시는 감사한 허수진 선배님, 좋은 실험 결과를 얻을 수 있게 도와주시고 조언과 응원을 해주시는 김길남 선배님, 꼼꼼한 실험과 옆에서 마음 깊이 도와주시는 안건내

선배님, 제브라피쉬 실험에 고민을 해결해주시고 잘 챙겨주시는 차선희  
선배님, 잘 될 수 있을 것이라고 응원을 아끼시지 않는 이승홍 선배님,  
멀리 캐나다에서 걱정해주시고 응원해주시는 강성명 선배님, 김아름다슬  
선배님, 여러 조언과 관심을 보여주시는 고석천 선배님, 연구계획서  
작성과 사소한 고민도 잘 들어주시고 해결해주시는 이원우 선배님,  
실험실에서 처음 들어와 아무것도 모르는 나에게 기초부터 실험을 잘  
가르쳐주시고 조언과 격려를 아끼지 않으시는 강민철 선배님, 여러  
분야에서 도움과 조언을 주시는 이지혁 선배님, 고주영 선배님, 처음  
제브라피쉬 가르쳐주신 고창익 선배님, 옆에서 항상 힘이 되어주고  
보살펴주는 나의 재영오빠, 착한 동기이자 많은 일을 함께한 고마운 나래,  
화이팅 넘치는 현수, 잘 적응하고, 앞으로 잘할 서영이, 저를 잘 따라주고  
많은 일을 도와주는 고마운 혜원이, 모든 일을 열심히 하는 윤택이,  
즐겁게 도와주셔서 감사한 은이언니, 사랑하는 후배인 형호, 바로,  
한국생활 잘 적응해 나가는 페르난도, 아산카, 왕퇴, 온건 이 모든 연구실  
식구들에게 감사의 마음을 전합니다.

언제나 나를 생각해주는 아름이 언니, 민영이, 뽀뽀로 동기 동휘오빠,  
승현이오빠, 처음 보는 학교후배이지만 조직실험 가르쳐주신 허성표  
박사님, 무척추방에 현실언니, 현기오빠, 희중오빠, 희도오빠 정말

감사합니다. 바쁘다고 대학원생활 내내 잘 챙기지 못해도, 여러 고민상담과 응원해주는 평생같이 할 나의 친구 예진이, 원지, 보경이, 슬이, 하의, 예술이 사랑하고 고마운 마음을 전합니다.

마지막으로 항상 힘이 되는 나의 부모님, 사랑이 가득한 가족 울타리에서 곱게 자란 작은 딸이 가족의 응원으로 박사졸업을 하게 되었습니다. 항상 바쁘다고 연락도 자주 안하고 집에도 잘 가지 않는 딸을 이해해줘서 감사하고 마음 놓고 공부할 수 있도록 원동력을 주셔서 감사하고 사랑합니다. 한결 같은 큰언니의 마음으로 다 받아주고 걱정해주는 내언니, 언니가 옆에 없었더라면 졸업이 힘들었을꺼야, 항상 내편이 되어주어서 고맙고 사랑합니다. 마지막으로 열심히 하고 노력하는 모습을 항상 보여줘서 걱정 없는 우리집 막내 남동생에게 사랑하는 마음을 전합니다.

다시 한번 더 저를 지금까지 지켜봐 주신 모든 분들께 감사하고 고마운 마음을 전합니다. 앞으로도 맡은 연구를 즐겁고 열심히 하며 진취적인 사람이 될 것이라 제 자신에게 다짐하며 이 글을 마칩니다.